# “Water Sensor for Testing Fluoride Concentrations in Groundwater to Improve Drinking Water Quality in Developing Countries”

by

Caitlin Vail

B.Sc., University of Alberta, 2017

A Thesis Submitted in Partial Fulfillment of the Requirements for the Degree of

MASTER OF APPLIED SCIENCE

in the Department of Civil Engineering



University of Victoria

"Water Sensor for Testing Fluoride Concentrations in Groundwater to Improve Drinking Water Quality in Developing Countries"

by

Caitlin Vail

B.Sc., University of Alberta, 2017

Supervisory Committee

Dr. Heather Buckley, Supervisor

Department of Civil Engineering

Dr. Peter Wild, Outside Member

Department of Mechanical Engineering

# Abstract

Excess fluoride in groundwater used for drinking can pose serious health hazards, especially in poor, rural areas of the developing world lacking water treatment. The World Health Organization recommends a maximum fluoride contaminant level of 1.5 mg/L in drinking water [1]. Over 200 million people in low- and middle-income countries currently drink groundwater over that limit [2]. Current field detection of fluoride typically uses HACH kits, with several groups developing smartphone based alternatives [3]. These methods are based on colorimetry. The HACH kit is limiting because appropriate training is required, results are sensitive to competing ion contamination and chlorine, the glassware must be clean, and repetition is needed to ensure reliability [4]. The use of a smartphone for in-field detection of fluoride is promising and takes a strong step towards quick, easy, reliable, and portable fluoride detection.

Our research takes the concept of a portable device one step further by using a fundamentally different, and simpler, mode of detection. We have demonstrated the use of optical fibers as an alternative, non-colourimetric fluoride detection method. The tip of a single mode optical fiber is coated with a thin film of Al and is immersed in an aqueous fluoride solution. The reaction between fluoride and the Al coating changes internal reflection proportional to fluoride concentration which is measured by a photodetector as an output voltage. We made great steps in optimizing the methods, materials, and code required for this sensor. Additionally, we built a device to allow approximate standardization of Al thickness as a function of the distance from the target and time of sputtering. We established the best practical thickness of Al coating, improved repeatability between sputter deposition events, and implemented an optical switch into the experimental set-up.

# Table of Contents

# List of Tables

**Chapter 2**



**Chapter 3**

# List of Figures

**Chapter 2**



**Chapter 3**

**Figure 4.06:** Illustration of the change in slope when the revised LabVIEW code is recording data compared to when it is not recording data. The recording data segments are steeper than the not recording data segments.

# Abbreviations

| ABBREVIATION | MEANING |
|---|---|
| Al | Aluminum |
| $F^-$ | Fluoride ion |
| WHO | World Health Organization |
| SPADNS | Sulfanilic acid azochromotrope, 2-(4-Sulfophenylazo)chromotropic acid trisodium salt |
| MOF | Metal-Organic Framework |
| ppm | Parts per million |
| SEM | Scanning electron microscope |
| VI | Virtual Instrument |

# Acknowledgements

I would like to acknowledge with respect the Lekwungen-speaking peoples on whose traditional territory the University of Victoria stands and the Songhees, Esquimalt and WSÁNEĆ peoples whose historical relationships with the land continue to this day.

I wish to thank all the people whose assistance was crucial in the completion of this project. The research in this thesis is funded by NSERC Discovery, CAMTEC, CFI-JELF, BCKDF, IESVic, CESAP, Electricity HR, UVic IRCPG, UNAC Greenspaces, and the Wighton Engineering Fund, as well as the Faculty of Graduate Studies at the University of Victoria.

I wish to show my sincere gratitude to my supervisor, Dr. Heather Buckley, for her guidance and support throughout this project; thank you for your encouragement, even when the road got tough. I am indebted to Dr. Peter Wild for taking the time to sit on my committee and for being an invaluable resource throughout my research; your time and expertise is greatly appreciated. I would like to pay my special regards to Dr. Jonathan Rudge for his technical expertise and insight; thank you for your unfaltering patience while training me on the equipment. Special thanks to Becky Hof, Geoff Burton, Kevin Jones, Arielle Garrett, and Armando Tura for the invaluable assistance you provided during my study.

I would like to recognize the encouragement I received from the Green Safe Water Group; thank you for your support, both moral and academic. Thank you to the coop students and high school student that have helped and furthered this research.

Thank you to my parents and brother for always being there to cheer me on and empower me.

It is with whole-hearted appreciation that I thank the above people without whom this milestone would not be possible.

# Chapter 1

## Introduction

Over 200 million people worldwide are drinking groundwater with fluoride concentrations over the World Health Organizations recommended maximum contaminant level of 1.5 mg F-/L in drinking water [1], [2]. This phenomenon is especially common in the African Rift Valley and parts of India, Sri Lanka, and Northern China [1], [2]. Regions that treat drinking water with fluoride have concentrations of 0.7 – 1.2 mg F-/L which is shown to have the beneficial effect of preventing dental caries, especially in children under 8 years of age [5]. Fluoride levels above the 1.5 mg F-/L recommended limit have the detrimental effect of causing dental and skeletal fluorosis, causing anemia, limb deformation, and chronic pain [5]. Communities that experience limited health care access and poor water treatment would benefit from a quick, easy, and cost-effective way of testing fluoride levels to determine whether a drinking water source is safe for consumption. Proper education and accessible water quality tests are paramount in empowering communities to make educated decisions about their water and in increasing public health.

## Background

*Current Fluoride Detection Methods*

Laboratory detection of fluoride in water is achieved by ion chromatography, ion-selective electrodes, or the SPADNS colorimetric method (using a red zirconium dye) [1]. In-field fluoride detection primarily uses HACH kits, which again use SPADNS dye. The colour change of the solution is proportional to the fluoride concentration [4]. However, results are very sensitive to small amounts of competing ion contamination, the glassware must be very clean, and repetition is needed to ensure reliability [4]. Use of the SPADNS method requires proper training. The reagent contains sodium arsenite and must be disposed of as hazardous waste [4].

*What is Needed*

For communities to address problems with water, they need to be able to measure the quality of the water. For a measurement technique to be useful in a low-income context, the following criteria are required:

- ease of usability,
- low probability of errors and low sensitivity of the results to those errors,
- quick time to output, and
- minimal amount of training required for operator to understand and act on the results.

Ideally, an operator would be able to go into the field and test a water source for fluoride with a small, portable device that outputs the results in a matter of seconds. Additionally, being able to give this device to someone in an at-risk community who has no scientific training and who can test for fluoride in water before drinking it would increase likelihood of market penetration and positive impact on the health of communities.

*Existing Solutions with Smartphones*

A literature review uncovered four articles published in the past four years that explore the use of Smartphones for quick, easy, reliable, and portable fluoride detection.

Levin [7] has demonstrated fluoride detection using a smartphone camera-affixed test chamber containing sample water and the reagent zirconium xylenol orange. The image captured by the camera is compared to pre-calibrated colours by the app, Akvo Caddisfly, which also uploads the information to a map. This method provides an untrained user with quick results at a low cost per test with an easily manufactured portable. However, the reagent generates hazardous waste, and distilled water is needed to keep the test chamber and camera adequately clean. Furthermore, the presence of chlorine in the sample water causes a false positive reading. Hussain [8] and Wen [9] have developed similar systems, which are compared in Table 1.

Vidal [3] have created a fluoride detection method that uses a micropaper-based analytical device (µPad) more reminiscent of universal pH paper. Coloured reagents and sample water saturate regions of the µPad, and a smartphone takes a picture of the µPad in a lightproof box. This method is portable, but again requires a liquid reagent.

*Existing Solutions without Smartphones*

A literature review uncovered two articles published in the past year that explore novel methods of in-field fluoride detection without the use of a smartphone.

Ebrahim et al., [10] have built a portable handheld device that tests for fluoride concentrations in groundwater using a metal-organic framework (MOF) [10]. This MOF-based solution uses a luminescent lanthanide MOF named SION-105 that detects fluoride through a lewis acid-base interaction between the fluoride ions present in the drinking and the active sites in SION-105 [10]. This method is sensitive to fluoride concentrations from 0.5 to 2 ppm F-, and the results are not affected by the addition of competing ions that are commonly found in water [10]. The device was used to test fluoride concentrations in water samples from three different countries and the results showed excellent agreement with the results found through ion chromatography [10]. Ebrahim et al., claim this fluoride detection device shows promise as a reliable, rapid, user-friendly process and is a viable contender with current in-field fluoride detection methods [10].

Thavarajah et al., [11] use a cell-free biosensor to detect the presence of fluoride above 2 ppm in groundwater samples [11]. This method uses a DNA template that encodes a fluoride sensitive riboswitch to control the transcription of downstream reporter genes so that the presence of fluoride activates protein and RNA reporter expression [11]. In other words, the presence of fluoride causes the riboswitch and reporter gene to produce a fluorescent or colourimetric output [11]. This method gives a binary presence/absence result if there is a fluoride concentration above 2 ppm or not, is robust to temperature variation, and is immune to competing ions [11]. Thavarajah et al., claim this method is cost-effective, easy, and field-deployable [11].

*Comparison of Fluoride Detection Methods*

Table 1.1. Comparison of In-Field Fluoride Detection Methods

| | Physical Form | Data Collected | Advantages | Reusability | Cost | Range | Limitations |
|---|---|---|---|---|---|---|---|
| **HACH Kit Pocket Colorimeter II, Fluoride (SPADNS II - Arsenic Free) [4]** | Colorimeter, reagent, deionized water, pipets and bulbs, thermometer, sample cells | $F^-$ conc. | Accurate, portable, established recognized method | Reagent must be replaced each test and AAA alkaline batteries must be replaced after they die | About 2000$CAD | 0.1-2ppm | Competing ions, clean glassware, training, **hazardous waste**, costly |
| **Levin [7]** | Smartphone, phone attachment, reagent | $F^-$ conc., GPS mapping | Quick, manufacturable parts, reagent readily available in market, portable, low training required, no need of technical expertise, ability to data transfer | Reagent must be replaced each test. | Expected to retail at 75USD without the phone and mapping system. Estimated cost of 0.3USD per test including reagent. | 0-2ppm | **Hazardous waste**, cleanliness, competing ion effects (specifically Chlorine) |
| **Hussain [8]** | Smartphone, phone attachment, reagent | $F^-$ conc., GPS mapping | Portable, quick, low training required, easy graphical interface, ability to data transfer | Reagent must be replaced each test. | Estimated cost of 206.23USD with reusable cuvettes | 0-2ppm | **Hazardous waste**, cleanliness of cuvettes, no information given on competing ion effects |

| | | | | | | | |
|---|---|---|---|---|---|---|---|
| **Wen [9]** | Smartphone, phone attachment, reagent | $F^-$ conc. | Portable | Reagent must be replaced each test. | No cost analysis done. Authors describe sensor as "low-cost" | 0.080-0.64ppm | **Hazardous** waste, scientific training required, low detection limit, no information given on competing ion effects |
| **Vidal [3]** | Smartphone, micropaper, reagent, lightproof box | $F^-$ conc. | Portable, user-friendly, micropaper is biodegradable | Reagent and micropaper must be replaced each test. | Estimated cost of 0.01USD per device. | 0.230-2.26ppm | **Hazardous waste**, training, equipment (ex. wax ink printer), time-intensive, no information given on competing ion effects |
| **Ebrahim [10]** | Portable device, SION-105 | $F^-$ conc. | Portable, quick, results are not impacted by competing ions, user-friendly, no re-calibration of the device is needed prior to measurement | SION-105 must be replaced each test. | No cost analysis done. | 0.5-2ppm | Lack of cost analysis, access to SION-105 |
| **Thavarajah [11]** | Portable device | Absence/ presence of $F^-$ above 2ppm | Portable, easy, results are not impacted by competing ions or temperature, results available in a matter of hours | DNA template must be replaced each test. | Estimated cost of 0.40USD per reaction. | Detects the presence of fluoride above 2ppm. | The sensor gives a binary present/absent result, it does not give the exact F- concentration. |

*Research Objectives*

This research further develops the smartphone idea and creates a reagent-free fluoride detection device. The objective of this project is to demonstrate that optical fibers are a reliable, reagent-free method for in-field fluoride detection, as well as determine the limitations of this method. Research includes improving standardization of the coating process, exploring the effects of different coating thicknesses on the optical fibers' performance, and implementing an optical switch into the experimental set-up.

This thesis comprises three manuscripts. In Chapter 2, the aluminum coating on the tips of the optical fibers is examined, and a fiber holder device is built to assist in the sputter deposition process. Chapter 3 explores the effects of the aluminum thickness on the tips of the optical fibers and the amount of time it takes for the output voltage to begin decreasing. We make recommendations on the optical aluminum thickness and future work. In Chapter 4 we implement an optical switch into the experimental set-up to increase the amount of data that can be collected, as well as draw observations on the impact of the optical switch on the results of the experiments.

This thesis presents a novel method of fluoride detection that brings the scientific community one step closer to achieving practical, rapid, and in-field fluoride detection.

# References


[1] "WHO guidelines for drinking water quality, Vol. 1. Recommendations," World Health Organization, Geneva, 2004.

[2] Eawag: Swiss Federal Institute of Aquatic Science and Technology, "Geogenic Contamination Handbook - Addressing Arsenic and Fluoride in Drinking Water," Dübendorf, Switzerland, 2015.

[3] E. Vidal, A. S. Lorenzetti, A. G. Lista, and C. E. Domini, "Micropaper-based analytical device (μPAD) for the simultaneous determination of nitrite and fluoride using a smartphone," *Microchem. J.*, vol. 143, no. August, pp. 467–473, 2018.

[4] HACH, "Fluoride SPADNS Method 8029." pp. 211–217, 2009.

[5] R. Liteplo *et al.*, "Environmental Health Criteria 227. Fluorides.," Geneva, 2002.

[6] H. L. Buckley, N. J. Molla, K. Cherukumilli, K. S. Boden, and A. J. Gadgil, "Addressing technical barriers for reliable, safe removal of fluoride from drinking water using minimally processed bauxite ores," *Dev. Eng.*, vol. 3, no. November 2017, pp. 175–187, 2018.

[7] S. Levin, S. Krishnan, S. Rajkumar, N. Halery, and P. Balkunde, "Monitoring of fluoride in water samples using a smartphone," *Sci. Total Environ.*, vol. 551–552, pp. 101–107, 2016.

[8] I. Hussain, K. U. Ahamad, and P. Nath, "Low-Cost, Robust, and Field Portable Smartphone Platform Photometric Sensor for Fluoride Level Detection in Drinking Water," *Anal. Chem.*, vol. 89, no. 1, pp. 767–775, 2017.

[9] Y. Wen, D. Kuang, J. Huang, and Y. Zhang, "Microaxicave colour analysis system for fluoride concentration using a smartphone," *RSC Adv.*, vol. 7, no. 67, pp. 42339–42344, 2017.

[10] F. Mish Ebrahim *et al.*, "Selective, Fast-Response, and Regenerable Metal−Organic Framework for Sampling Excess Fluoride Levels in Drinking Water," *J. Am. Chem. Soc.*, vol. 141, no. 7, pp. 3052–3058, 2019.

[11] W. Thavarajah, A. D. Silverman, M. S. Verosloff, N. Kelley-Loughnane, M. C. Jewett, and J. B. Lucks, "Point-of-Use Detection of Environmental Fluoride via a Cell-Free Riboswitch-Based Biosensor," *ACS Synth. Biol.*, vol. 9, no. 1, pp. 10–18, 2020.

# Chapter 2

*Manuscript Title*

Fiber Holder to Assist in Sputter Deposition Coating of Optical Fibers

*Authors*

C.A. Vail, G. Burton, P.M. Wild, H.L. Buckley

*State of Publication:*

This manuscript has been accepted as a Paper to the *2nd International Conference on New Horizons in Green Civil Engineering* which entails a four-page limit; there is no limitation on the number of display items (i.e., figures and tables) for this submission.

*Author Contributions:*

C.A. Vail, P.M. Wild, and H.L. Buckley conceived the structure of the fiber holder. G. Burton constructed the fiber holder and created the engineering drawings. C.A. Vail performed the laboratory experiments and carried out the analysis of the results. C.A. Vail, P.M. Wild, and H.L. Buckley contributed to the interpretation of the results. C.A. Vail wrote the manuscript and H.L. Buckley performed revisions and gave critical feedback. H.L. Buckley secured the funding for this research.

## Abstract

Sputter deposition is used to coat 100 nm of aluminum (Al) on the distal tips of single mode optical fibers. A fiber holder was built to secure the fibers in the sputter deposition chamber with their tips facing the aluminum target while being sputter coated. Our findings show that the distance between the target and the tips of the optical fibers has a large effect on the Al thickness of the coating. The goal of the fiber holder is to maximize repeatability of the sputter deposition by ensuring the fibers are held in the same position every time sputter deposition occurs. We expect increased repeatability between tests when using the fiber holder with during sputter deposition.

## Keywords

- Sputter deposition
- optical fibers
- holder

## Introduction

Magnetron sputtering, a deposition technology for thin-films, can be traced back to the 19$^{th}$ Century to Grove's observations of pulsed diode sputtering [1]. In the past two decades, sputter deposition has been used to deposit thin-films onto surfaces, analyze trace impurities of materials, treat and process surfaces, and numerous other technological applications [2]. This paper does not review the history or latest developments of magnetron sputtering, which is a mature and widely used industrial technology and is reviewed elsewhere [1]. Most commonly, sputter deposition is used in industry for large-area deposition of thin films however, magnetron sputtering is a flexible and scalable technique that can be used for a wide range of thin film deposition [2]. We use magnetron sputtering for an uncommon application: coating the tips of single-mode optical fibers with thin films (up to 100 nm) of aluminum. In doing so, our goal is to develop a sensor to detect fluoride concentrations in groundwater [3]. Common materials to be coated would be able to lay flat across the top of the substrate within the sputter deposition chamber. The substrate is where the material goes that is to be coated with a thin film, and the target is the material which coats the substrate. We need the tips of the optical fibers to be perpendicular to the surface of the target, meaning the fibers cannot lay across the top of the substrate. For this reason, we have designed a fiber holder.

Sputter deposition uses a vapor-based physical deposition method [4]. As shown in Figure 2.01, particles are removed from the surface of a target through ion bombardment [1]. The released particles condense on the surface of the substrate, creating a coating [1].

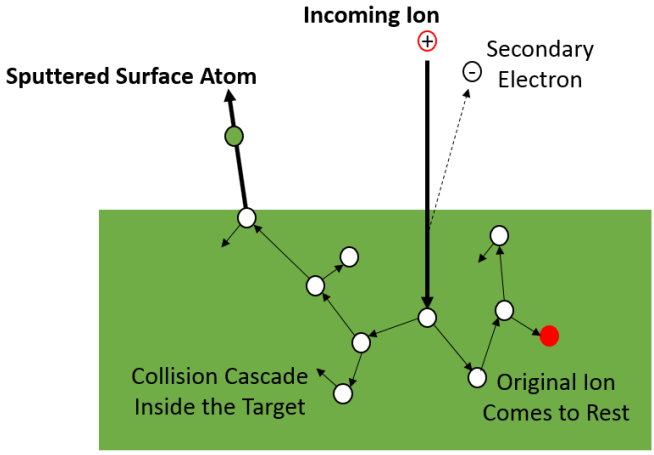


Figure 2.01: Ion bombardment of Argon ions bombarding the target surface releasing surface atoms and secondary electrons into the plasma, adapted from [1].

Factors such as the number of particles removed off the surface of the target, penetration depth of incoming ions, and nature of the collisions are influenced by the mass and energy of ions and the characteristics of the target material [1]. As the name suggests, a magnetron is used to create a magnetic field [1]. This allows electrons released from the target to perform numerous gyrations along magnetic field lines thus forcing electrons to travel a longer path in front of the magnet [1].

Energetic electrons collide with process gas atoms, effectively ionizing them and creating a plasma which consists of both electrons and ions [1]. The plasma and its boundaries determine the local electric field [1]. The positive ions are attracted to the target, which is negatively charged, and continue sputtering the target [1]. Sputtered atoms travel to the substrate to coat it with a thin film [1]. Substrate temperature and energy of the atoms determine the microstructure of the thin film coating [1]. In practical operation, process parameters for sputtering are limited and consist primarily of controlling the substrate temperature, the gas pressure, and the time of operation [1]. This process is illustrated in Figure 2.02.

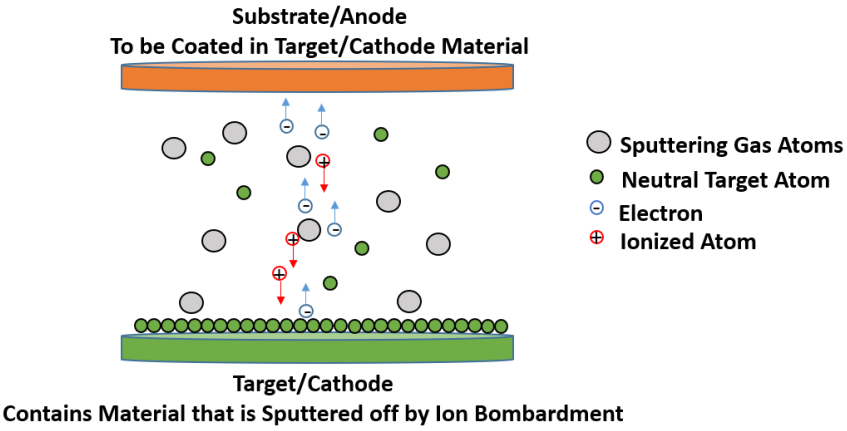


Figure 2.02: Sputter Deposition Process

An additional process parameter that can be controlled is the distance between the substrate and the target, which has a strong effect on the distribution and characteristics of the deposition molecules [5]–[8]. As the distance between the substrate and the target increases, the uniformity of the distribution of

the depositing atoms increases however, the kinetic energy of the depositing atoms decreases [5]. Furthermore, the substrate-target distance has an effect on the deposition rate, as well as the microstructure and hardness of the thin-film coating [5].

This paper does not give an extensive review on the underlying physics of magnetron sputtering as entire books have been written on the subject [9]. Rather, the goal is to explain how the fiber holder we have built compliments sputter deposition to make it a more robust, reliable, and repeatable process for coating an unconventional object like an optical fiber.

## Design

In this research we use a Mantis QUBE sputter deposition machine (Mantis Deposition-UK). The fiber holder is designed to hold up to 17 single-mode optical fibers in a vacuum-sealed chamber under $10^{-3}$ mbar pressure. As shown in Figure 2.03, the fiber holder consists of a ring to lay atop the substrate, threaded rods, and a bottom portion containing clamping heads and an O-ring clamp that holds the fibers in place.

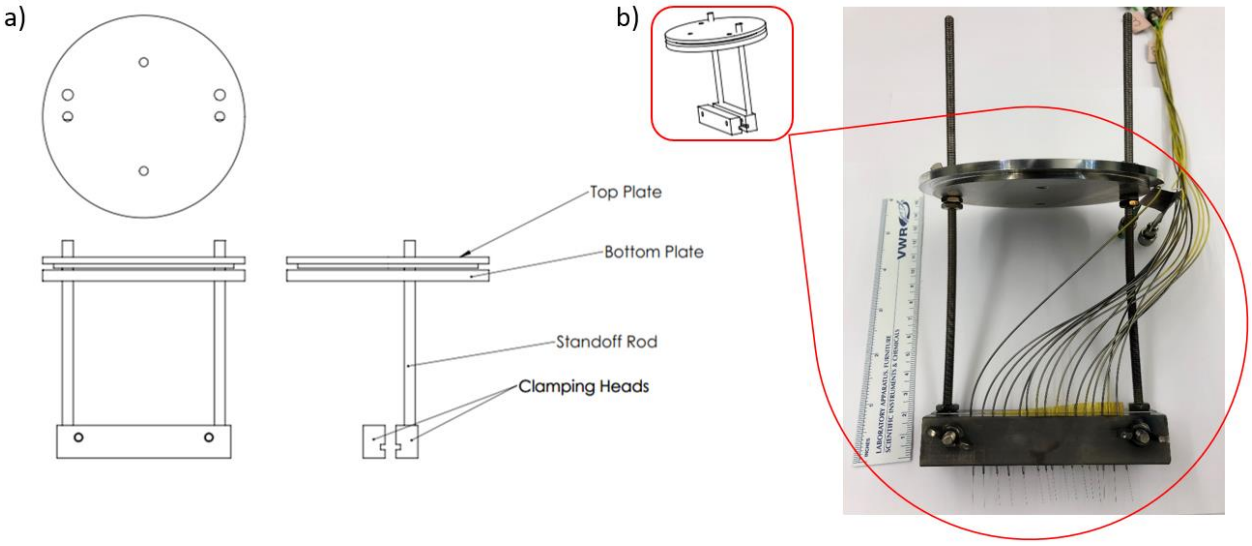


Figure 2.03: a) Engineering Drawings. The side view depicts the substrate consisting of the top plate and bottom plate, the rods going down, and the two clamping heads which squeeze the fibers. The front view shows the substrate at the top, the two rods going down, and the clamp at the bottom with two holes where rods protrude allowing fasteners to hold the two clamping heads together. The top view depicts the top plate with holes where the two rods may be positioned to go through depending on the desired positioning. B) Photo showing the fiber holder securing 17 fibers with 3 mm between each fiber. The fibers are secured with vacuum tape to help hold them in place. The substrate in this photo only uses the top plate as we found the bottom plate was not necessary; the top plate ensures enough stability on top of the substrate so the fiber holder does not move.

The materials were chosen based on what can be exposed to plasma for a long period of time, meaning non-magnetic materials are required so the magnetic and electric fields created by the plasma and magnetron are not affected. Moreover, no material containing pockets of air, such as foam or wood, can be used because those pockets would compromise the vacuum state of the chamber. Table 2.1 summarizes the materials used to build the fiber holder.

Table 2.1: Fiber Holder Materials

| PIECE | MATERIAL |
|---|---|
| Top Plate and Bottom Plate | Aluminum 6061-T6 |
| Threaded Rods | Unmagnetized Stainless Steel 18-8 |
| Clamping Heads | Aluminum 6061-T6 |
| Fasteners | Unmagnetized Stainless Steel 18-8 |
| O-Ring Clamp | Viton |

The O-ring clamp made from Viton is inside the clamping heads, as shown in Figure 2.04. Its purpose is to prevent the fibers from slipping. The parts and labor to build this fiber holder cost $200 CAD in total to produce a single fiber holder. The mass production of several fiber holders would decrease the cost of each individual fiber holder.

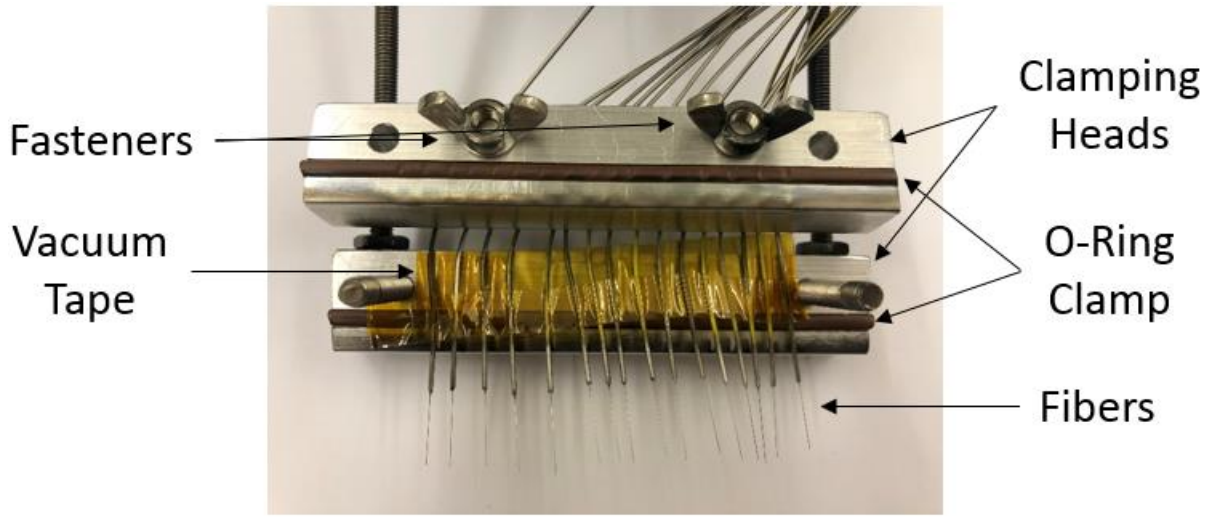


Figure 2.04: Close up of the clamping mechanism. 17 fibers are secured with vacuum tape with at least 3 mm between each fiber. The O-ring clamp is the viton material (rubber looking stripe) across the aluminum clamping heads. Stainless steel fasteners secure the two clamping heads together; the fibers are squished between the two clamping heads.

The threaded rods are adjustable, a major advantage to this design because it allows the user to adjust the distance between the fiber tips and the target. The closer the tips of the fibers are to the target, the more direct and concentrated the stream of sputtered atoms will be. The further away the tips of the fibers are from the target, the broader the array of sputtered atoms are, and the higher the likelihood that the fibers will be evenly coated. Additionally, the rods may be bent so the fibers are perpendicular to the target surface, effectively allowing the tips to be facing the oncoming stream of sputtered atoms. The

fiber holder may be rotated atop the substrate so the fiber tips are perpendicular to any of the targets, of which there are four in a Mantis QUBE sputter deposition machine. This increases the versatility of the fiber holder because it may be used in conjunction with any of the targets in the chamber; however, the user must be conscious of making sure the fiber holder is rotated atop the substrate in the same position between sputter deposition events. Figure 2.05 shows the fiber holder.

Overall, the fiber holder increases the parameters we can control of the sputter deposition process, fixing the fibers perpendicular to the surface of the target and at a set vertical distance from the surface of the target.

## Sample and Instrument Operation

Pigtail FC/APC SM SX Ø0.9 1M (Product #14152, FS.com-China) single mode optical fibers are used in all experiments. These single mode optical fibers are 1 meter long with one end having a ferrule connector (FC) and the other having an angle polished connector (APC). The fibers consist of a jacket made from yellow polyvinyl chloride (PVC) plastic with a diameter of 0.9 mm, a coating underneath the jacket with a 0.25 mm diameter,  0.125 mm diameter cladding, and the core of the fiber which has a diameter of 0.009 mm [10]. The single mode optical fibers are stripped of their jacket and coating for about 3 cm from the distal end. About 1.2 cm of the distal end of the optical fiber is cleaved with a High Precision Fiber Cleaver (Fujikura), and the exposed optical fiber is cleaned with acetone. Securing the fibers into the holder is best assisted with vacuum tape to ensure they do not slip out of place. A new piece of vacuum tape is applied to the holder each time. We leave 3 mm between each fiber. Once the fibers are in place, we clamp the second bottom piece with fasteners, so the O-ring helps grip the fibers in their desired position as shown in Figure 2.04. Now the fiber holder may be inserted into the sputter deposition chamber as shown in Figure 2.05. The top circular substrate of the fiber holder is slid on top of the substrate in the chamber. The fiber holder can be twisted so that the tips of the optical fibers are perpendicular to the surface of the target. The rods are made of 18-8 Stainless Steel and can in practical use be bent to better position the tips of the optical fibers perpendicular to the surface of the target; however, this compromises the ability to adjust the rods height. At this stage, the machine can be sealed for sputter deposition.

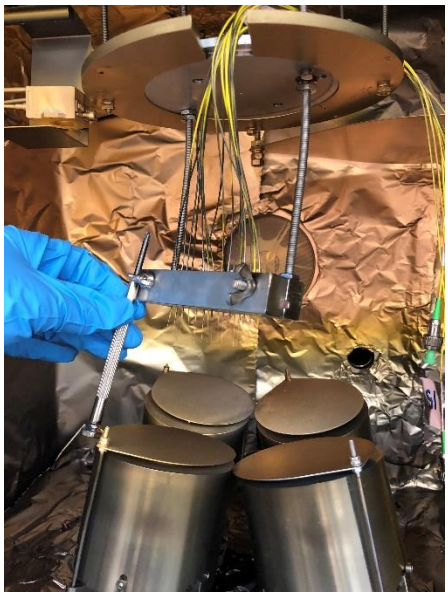

Figure 2.05: Fiber holder mounted on the substrate in the chamber of a Mantis QUBE sputter deposition machine with fibers pointed towards the intended target.

In our tests, we use the sputter deposition machine (QUBE, Mantis Deposition-UK) to coat single-mode optical fibers with a thin-film of aluminum. Argon gas is used as the sputtering gas however, nitrogen gas is used to vent the chamber (introduce air into the chamber so the door opens). The argon gas is pumped into the chamber at a flow of 35 sccm (standard cubic cm per minute), power applied is 60 W, and the pressure in the chamber once under vacuum is $10^{-3}$ mbar. The temperature at the bottom of the chamber is 28°C, at the bearing is 27°C, and at the motor is 26°C. The Mantis QUBE uses a 13.56 MHz generator.

## Results

In each application of the fiber holder, we coat 17 single-mode optical fibers using the fiber holder with the sputter deposition machine. To calibrate the system, we fixed a 1 $cm^2$ piece of glass to the fiber holder such that the glass is held at the same position as the tips of the optical fibers so that the distance between the target the piece of glass is the same as the distance between the target and the tips of the optical fibers. We sputter coated the optical fibers and the glass slide with Al. The internal calibration of the sputter deposition machine estimated the Al coating thickness at the substrate (30 cm away from the target) to be 10 nm. Using a profilometer (DektakXT Stylus Profiler, BRUKER), we measured the Al thickness on the glass (10 cm away from the target) to be 100 nm.

## Discussion

Our observations indicate that the distance between the target and the tips of the optical fibers may have a large effect on the thickness of the Al coating. The large inter-sample variability in some aspects of the data we observed in our early work [3] may be explained by variation in positioning of the fibers relative to the target both between and within instances of sputter coating of fibers. We expect the use of the fiber holder to be key in ensuring repeatable and reliable data for our research moving forward because it will increase the consistency of the Al thickness on the tips of the optical fibers each time we sputter coat.

The sample holder concept with the same materials can be applied to other sputter deposition machines using various target materials, sputtering gases, chamber pressures, and temperatures. Furthermore, the fiber holder can be used outside the scope of single-mode optical fibers and can hold in place any object that fits within the clasp. An alternate shape of clamp could readily be custom designed to hold the faces of other unusual objects perpendicular to the target.

The holder increases control over the process parameters of sputter deposition, namely, specifying placement within the chamber. This decreases the number of variables to consider when analyzing samples prepared by sputter deposition. Through adjusting the distance between the surface of the target and the tips of the optical fibers, further control over the nature of the thin film coating is achieved.

## Conclusions and Outlook

The fiber holder we have designed and built is sturdy, simple to use, and able to hold up to 17 single-mode optical fibers at once in a Mantis QUBE sputter deposition machine. It can be adjusted to hold the fibers closer or further away from the target and thus accommodates the desired outcome of the user. Furthermore, the fiber holder may be rotated atop the substrate to accommodate the use of any of the targets in the chamber. Future work may include introducing a clamp or a notch to set the device atop the substrate so it does not rotate, should the user wish to have the fiber holder sit in the same position for subsequent instances of sputter deposition, rotated at the same angle towards the target. Moreover, other future work may include building two sets of clamping mechanisms in a fiber holder so that double the number of fibers may be sputter coated at once. However, even in its current iteration, the fiber holder achieves the goal of substantially increasing repeatability between applications of the sputter deposition machine, improving the quality control on output coated fibers.

## Acknowledgements

The authors would like to thank Dr. Jonathan Rudge of the Centre for Advanced Materials and Related Technology (CAMTEC) for advising on appropriate materials to use in the fabrication of the fiber holder, as well as his support regarding the use of the sputter deposition machine and profilometer. Additionally, the authors would like to thank coop student Sydney Hoffman for assisting C.A. Vail with laboratory work using the sputter deposition machine and profilometer.

For financial support the authors would like to thank NSERC Discovery, CFI JELF, BCKDF, IESVic CESAP, UNAC GreenSpaces, Electricity HR, UVic IRCPG, and the Wighton Engineering Fund.

# References


[1] A. Anders, “Tutorial: Reactive high power impulse magnetron sputtering (R-HiPIMS),” *J. Appl. Phys.*, vol. 121, no. 17, 2017.

[2] D. Depla and S. Mahieu, *Reactive Sputter Deposition*. 2008.

[3] V. Moradi, E. A. Caws, P. M. Wild, and H. L. Buckley, “A simple method for detection of low concentrations of fluoride in drinking water,” *Sensors Actuators, A Phys.*, vol. 303, 2020.

[4] D. Lundin and K. Sarakinos, “An introduction to thin film processing using high-power impulse magnetron sputtering,” *J. Mater. Res.*, vol. 27, no. 5, pp. 780–792, 2012.

[5] R. Wuhrer and W. Y. Yeung, “Effect of target-substrate working distance on magnetron sputter deposition of nanostructured titanium aluminium nitride coatings,” *Scr. Mater.*, vol. 49, no. 3, pp. 199–205, 2003.

[6] P. J. Kelly and R. D. Arnell, “Magnetron sputtering: A review of recent developments and applications,” *Vacuum*, vol. 56, no. 3, pp. 159–172, 2000.

[7] M. Yusupov, E. Bultinck, D. Depla, and A. Bogaerts, “Behavior of electrons in a dual-magnetron sputter deposition system: A Monte Carlo model,” *New J. Phys.*, vol. 13, 2011.

[8] M. Ohring, “Materials Science of Thin Films,” in *Materials Science of Thin Films Deposition & Structure, 2nd ed.*, Second Edi., vol. 1, no. 2001, Academic Press, 2002, pp. 106–117.

[9] R. Behrisch and W. Eckstein, *Sputtering by Particle Bombardment: Experiments and Computer Calculations from Theshold to MeV energies*, vol. 110. 2007.

[10] FS.com, “Customized LC/SC/FC/ST/LSH Simplex OS2 Single Mode Fiber Optic Pigtail #14152.” [Online]. Available: https://www.fs.com/products/14152.html. [Accessed: 14-Aug-2020].

# Chapter 3

*Manuscript Title*

Development of a Thin-Film Aluminum Coating on the Tip of an Optical Fiber for the Detection of Fluoride in Groundwater

*Authors*

C.A. Vail, V. Moradi, E.A. Caws, P.M. Wild, H.L. Buckley

*State of Publication:*

This manuscript is intended to be submitted as a Journal Article in the *Journal of Sensors and Actuators A: Physical*. It requires additional data collection before submission.

*Author Contributions:*

H.L. Buckley, P.M. Wild, and V. Moradi conceived the concept of the fluoride sensor. V. Moradi and E.A. Caws carried out the initial laboratory experiments. V. Moradi, E.A. Caws, P.M. Wild, and H.L. Buckley contributed to the interpretation of the initial experiments' results and published the results: V. Moradi, E. A. Caws, P. M. Wild, and H. L. Buckley, "A simple method for detection of low concentrations of fluoride in drinking water," *Sensors Actuators A Phys.*, p. 111684, 2019. C.A. Vail carried out further laboratory experiments and performed statistical analysis of the data. C.A. Vail, P.M. Wild, and H.L. Buckley contributed to the interpretation of the results. C.A. Vail wrote the manuscript; H.L. Buckley provided critical revisions and feedback. H.L. Buckley secured the funding for this project.

## Abstract

Groundwater used for drinking containing fluoride levels above 1.5 mg/L, as per the World Health Organization's maximum fluoride contaminant level, poses serious health hazards [1]. Current field detection methods of fluoride are based on colorimetry and have several limitations. Our research demonstrates the use of optical fibers as an alternative, non-colourimetric fluoride detection method. The cleaved distal tip of a single mode optical fiber is coated with a thin film of Al and is immersed in an aqueous fluoride solution. The reaction between fluoride and the Al coating changes internal reflection, giving a rate change of voltage at a photodetector proportional to fluoride concentration. We have observed a strong relation between Al thickness and the amount of time required for the output voltage to begin decreasing. In [2], we created a fiber holder to increase standardization of Al thickness as a function of the target to fiber tip distance and the duration of sputtering time. In this manuscript, we establish the best practical thickness of Al to optimize activation time and perform a statistical analysis of fluoride concentration and rate change of voltage.

## Keywords

- Drinking water
- Fluoride
- Sensor
- Optical Fibers

## Introduction

The World Health Organization recommends a maximum contaminant level of fluoride of 1.5 mg F-/L in drinking water [3]. Over 200 million people in developing countries drink groundwater over that limit, most notably in the African Rift Valley and parts of India, Sri Lanka, and Northern China [1], [4]. Regions that add fluoride to treated drinking water typically add concentrations of 0.7-1.2 mg/L of fluoride [5]. This has the beneficial effect of preventing dental caries, especially in children under the age of 8 [5]. Unsafe levels of fluoride in water cause problems with skeletal tissue, ranging from anemia and dental fluorosis to debilitating skeletal fluorosis including limb deformation and chronic pain [5].

The World Health Organization published in their 2004 *Drinking Water Guidelines* that "in some regions, it has been shown that investments in water supply and sanitation can yield a net economic benefit, since the reductions in adverse health effects and health care costs outweigh the costs of undertaking the interventions," and "safe water favours the poor in particular… and can be an effective part of poverty alleviation strategies" [1]. In communities with limited health care access and poor water treatment, having a quick, easy, and cost-effective way of testing the fluoride level to determine whether a drinking water source is safe or not is a step in increasing public health. Proper water quality tests and education on the effects of fluoride allow organizations to allocate resources and in turn empower communities to make decisions about their water.

## Background

*Use of Optical Fibers in Sensors*

The year 1960 marked the invention of the laser followed shortly by the development of the modern low-loss optical fiber in 1966 [6]. The initial usage of optical fiber technology was in telecommunications, but the past half century has seen an enormous expansion in its application [6]. The first experiments using optical fibers in a sensor date back to the early 1970's with initial development occurring in the fields of

magnetic, temperature, pressure, acceleration, current, fluid level, strain, and displacement sensing [6]. Today, many new sensing mechanisms that use optical fiber technology are emerging such as fiber laser-based sensing, photonic crystal fiber sensors, liquid crystal photonics, micro/nano-fiber sensing, surface plasmon resonance sensors, Bragg gratings in silica and polymer fibers, and interferometric fiber sensors [6]. The widespread development of optical fiber sensing technology is opening many doors for new applications.

*Modified Optical Fibers for Reagent-Free Fluoride Detection*

Despite the extensive development of optical fiber sensing technology, a preliminary literature review discovered only two articles that use optical fiber technology to detect fluoride concentrations in groundwater, and one of those articles is published by our research team [7], [8]. The one other optical fiber technology used to detect fluoride concentrations uses a fiber Bragg grating developed from the fabrication of photosensitive fibers through phase mask technique to detect fluoride concentrations in drinking water ranging from 0.05 – 8 ppm [7]; our approach is fundamentally different [8]. Most other simple methods for fluoride detection are colourimetric and make use of chemical reagents [9]–[13].

In our previous work [8], the tip of a single mode optical fiber was coated with 35 nm of aluminum via sputter deposition. The optical fiber was then immersed in an aqueous fluoride solution and 1550 nm wavelength light was shone down the optical fiber. The reaction between fluoride and aluminum destroys the aluminum coating thus affecting the reflection of light to the detector as shown in Figure 3.01. The reflected light from the tip of the optical fiber sensor is translated by the photodiode into an output voltage. A data acquisition system translates this to digital data read by a PC. The voltage decreases as the fluoride reacts with aluminum. This preliminary work indicated that the rate change of output voltage was proportional to fluoride concentration up to 5 mg/L of fluoride.

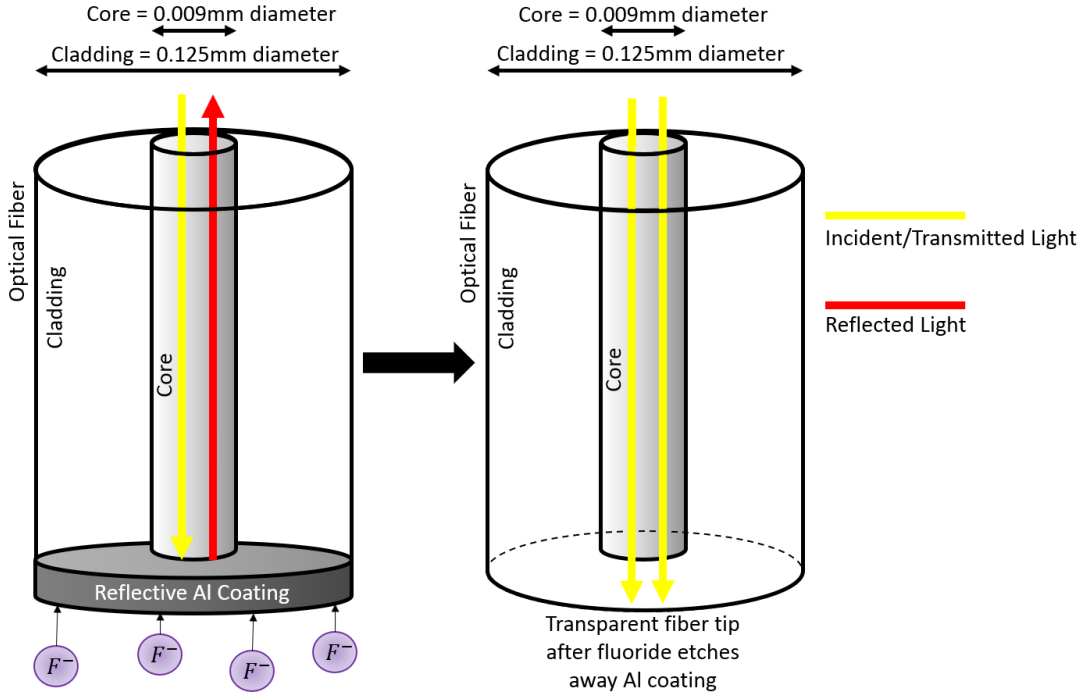


Figure 3.01. Light interacting with an aluminum coated optical fiber tip before and after exposure to fluoride in water as modified from [8].

*Research Objectives*

This research uses optical fibers to create a reagent-free fluoride detection device. The objective is to improve the fluoride sensor demonstrated in Moradi et al., 2019 [8] and determine its limitations. We do so by exploring two hypotheses. The first hypothesis is that the thickness of the sputter deposited Al coating on the tips of the optical fibers impacts the time required for the output voltage to begin decreasing. The thicker the Al coating, the longer the wait time is to reach a critical threshold thickness of Al coating and for the output voltage to begin decreasing, as shown in Figure 3.02. Based on this relationship, we make recommendations on the optimal Al thickness for further studies of the system. We experienced inconsistent wait times ranging from hours to days before the output voltage began decreasing; finding the optimal Al thickness is important for time efficiency. The second hypothesis, which was previously demonstrated in [8] but requires validation under more controlled initial coating thickness conditions, is that the fluoride concentration in the water samples impacts the rate change of voltage, shown in Figure 3.03. This relationship will determine the accuracy and precision with which the sensor detects fluoride concentrations.

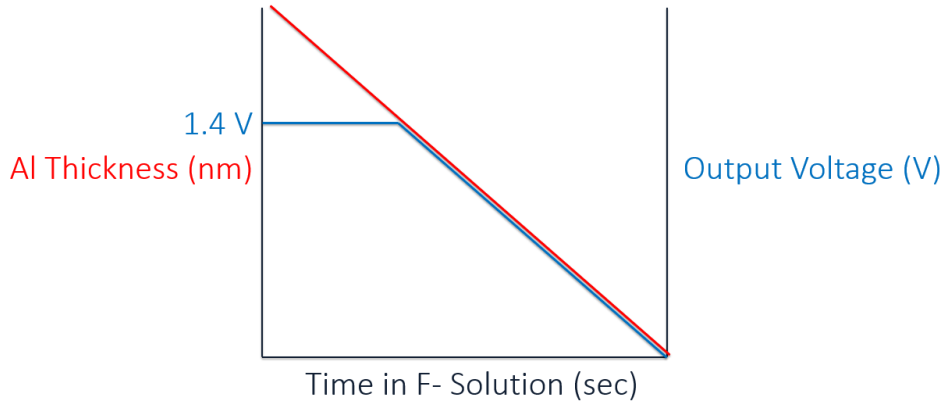


Figure 3.02: Illustration of the trend between Al thickness and activation time. The thicker the Al coating, the longer the activation time.

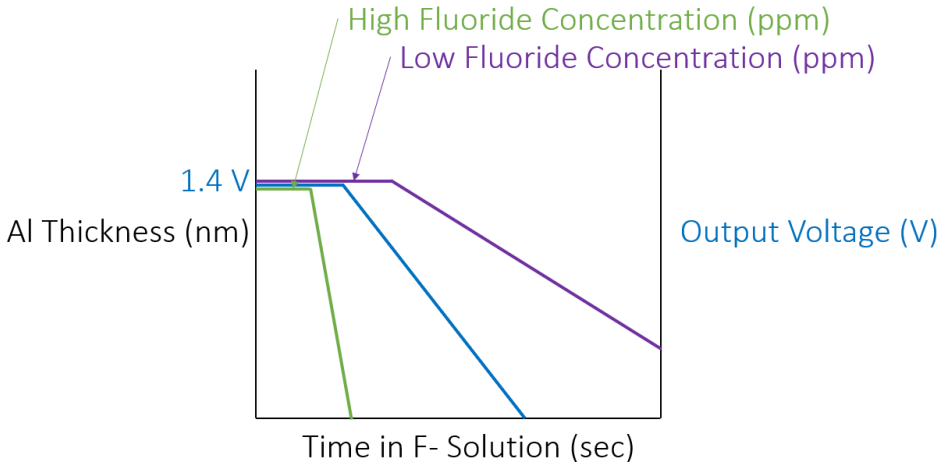


Figure 3.03: Illustration of the trend demonstrated in Moradi et al., 2019 [8] that fluoride concentration in the water sample impacts rate change of voltage.

## Methods and Materials

*Fibers and Preparation*

The optical fibers used in our experiments are labelled 9/125 OS2 Single Mode Fiber Optic Pigtail Yellow – 1M FC/APC Simplex PVC Φ 0.9 mm (Product #14152, FS.com-China). Simply put, they are one meter long single mode optical fibers with one end having a ferrule connector (FC) and the other end having an angle polished connector (APC). The ferrule connector is made out of zirconia ceramic and the angle polished connector means that the tip of the fiber is polished to have an angle [10]. The jacket protecting the fiber is made of yellow polyvinyl chloride (PVC) plastic and has a diameter of 0.9 mm [10]. Underneath the jacket is a 0.25 mm coating, a 0.125 mm cladding, and the core of the fiber which has a diameter of 0.009 mm [11]. The fiber grade is G.657.A1 and has an insertion loss (IL) ≤ 0.3 dB and a return loss (RL) ≥ 60 dB [11]. The specifications of the optical fibers are shown in figure 3.04.

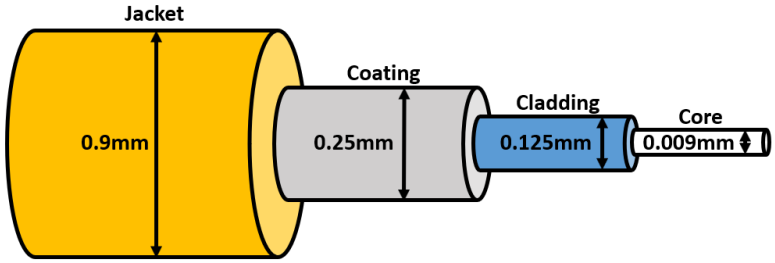


Figure 3.04: Schematic illustrating the components of the single mode optical fibers. The jacket has a diameter of 0.9 mm and is made of yellow PVC plastic. The coating has a diameter of 0.25 mm, the cladding has a diameter of 0.125 mm, and the fiber core has a diameter of 0.09 mm.

The jacket and coating were stripped from about 3 cm from the distal end of the fibers. A cleaver (High Precision Fiber Cleaver, Fujikura) was used to cleave 1.2 cm of the distal end of the fiber. The same cleaver was used across all experiments. The exposed optical fiber core was then cleaned with acetone. The fibers were secured in the fiber holder with the assistance of vacuum tape [2]. The purpose of the fiber holder was to secure the fibers in the sputter deposition chamber so the fiber tips were perpendicular to the target at a set distance from the target [2]. The fiber holder increased the repeatability between sputter deposition events because it ensured the fiber tips were the same distance from the target each time the fibers were sputter coated [2]. Up to 17 fibers were secured in the fiber holder at once with at least 3 mm between each fiber [2].

*Sputter Deposition and Profilometer*

The exposed tip of the optical fiber was sputter coated (QUBE, Mantis Deposition-UK) with aluminum to a specified thickness. First, the sputter deposition chamber is vented using nitrogen gas at a flow of 35 sccm (standard cubic cm per minute) at an applied power of 60 W. The same target holder should be used for all sputter deposition events; in our experiments we use target holder #2. The fiber holder (with the fibers) is placed inside the chamber atop the substrate, with the fiber tips perpendicular to the Al target. The chamber is sealed to a vacuum state of $10^{-3}$ mbar. Argon gas is used as the sputtering gas, and it pumps into the chamber at a flow of 35 sccm at an applied power of 60 W. The sputter deposition machine is controlled by a program called TITANIUM. The TITANIUM program tells the sputter deposition machine what to do; it sputter deposits the Al until the software indicates the input thickness is reached. It is important that the Argon gas flow and the RF supply are set to the same specifications at each sputter deposition event as those parameters affect the thickness of the sputtered thin film and are not accounted for in the software calibration. In our experiments, we set the Argon gas flow to 15 sccm and the RF supply to 175 W. While sputtering, a water chiller controls the temperature of the machine; the temperature at

the bottom of the chamber is 28°C, at the bearing is 27°C, and at the motor is 26°C. When the specified Al thickness is reached, the TITANIUM program shuts the machine down, and the chamber is ready to be vented and the samples removed.

We used a profilometer (DektakXT Stylus Profiler, BRUKER) to measure the actual deposited Al thickness and compare it to the desired Al thickness that was input into the TITANIUM program. We fixed a 1 $cm^2$ piece of glass to the fiber holder such that the glass was held at the same distance from the target as the tips of the optical fibers. The thickness of the Al coating on the piece of glass was checked in 6 or 7 spots, and the average of those thicknesses was taken and reported as the actual Al thickness. The actual Al thickness was then compared to the intended Al thickness.

*Light Microscopy and SEM*

We used a Cytation 5 Plate and Image Reader (BioTek Cytation 5 Cell Imaging Multi-Mode Reader) to take microscope images of the tips of the optical fibers from a side view. Additionally, a scanning electron microscope (SEM) (Hitachi S-4800 FESEM) was used to take images of the tips of optical fibers looking face-on at the top.

*Solution Preparation*

Test solutions were prepared using distilled water and sodium fluoride (NaF > 0.99) (Sigma Aldrich). To prepare a 100 mg/L stock solution of fluoride, 221 mg of NaF was dissolved in 1 L of distilled water. The stock solution was diluted to prepare the desired concentrations for the test solutions. To make a 10 mL solution of 5 ppm F- solution using deionized (DI) water, 0.5 mL of the 100 mg/L stock solution of fluoride is pipetted into a plastic 15 mL centrifuge tube followed by 9.5 mL of DI water. This solution has a pH of 7 and an ionic strength of 0.263 mmol/L. A 10 mL solution of 1 ppm F- solution using DI water is made by pipetting 0.1 mL of 100 mg/L stock fluoride solution and 9.9 mL of DI water into a plastic 15 mL centrifuge tube. This solution has a pH of 7 and an ionic strength of 0.0526 mmol/L. We began our experiments with 5 ppm fluoride solutions with a pH of 7 and an ionic strength of 0.263 mmol/L as a benchmark to judge the sensitivity of the sensor.

*Experimental Set-Up and Instrumentation*

As shown in Figure 3.05, for one set of experiments, the coated fiber tips are immersed in the test solutions. The broadband light source (BBS 1550, AFC Technologies) emits 1550 nm light that is transmitted through the optical splitter (BRR-35S, Blue Road Research Inc.) to the optical switch (Fiber-Fiber 1x32 Optical Switch Box, Agiltron). The optical switch channels the light to the coated fiber tips; the switch allows up to thirty-two fibers to be run simultaneously, but for the purposes of our experiments, we run up to eight fibers per set of experiments; on each fiber, data is recorded for 5 second intervals before cycling through the others in the set. Light reflected from the fiber tips is transmitted back through the fibers, optical switch, optical splitter, and to the photodiode (FDP 510, MenloSystems). The photodiode produces voltage proportional to the intensity of reflected light, which is transmitted to the data acquisition (DAQ) module (NI USB-6008, National Instruments) at a rate of 10 Hz. The DAQ module converts the output voltage, which is an analog signal, to a digital signal, which is then read by the PC.

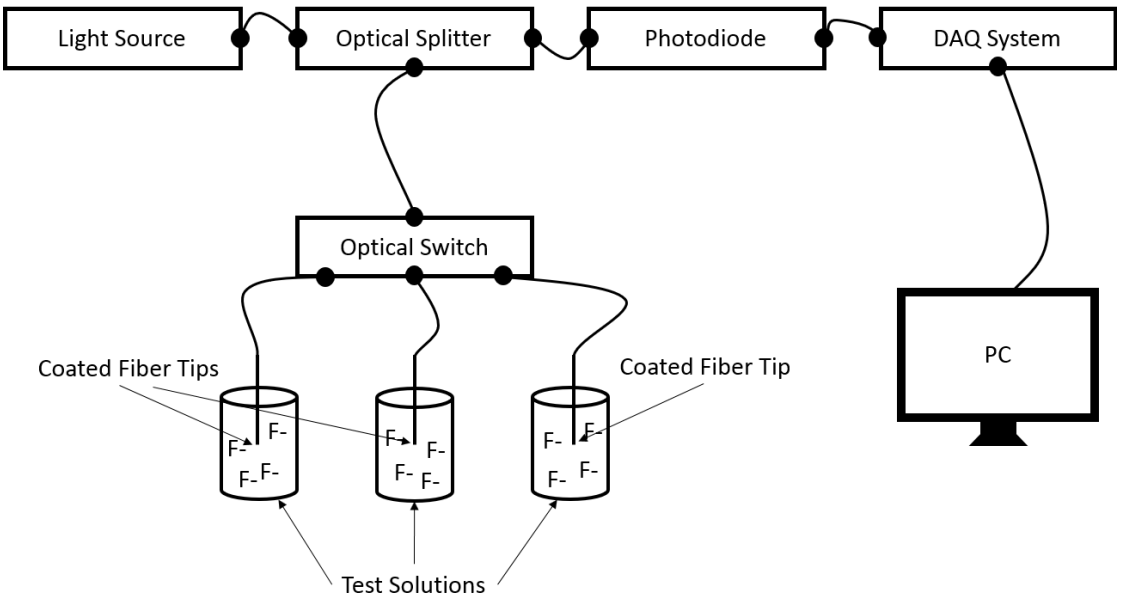


Figure 3.05: Schematic drawing of the experimental set-up as modified from [8].

*Test Procedures*

Each fiber tip was used in a single solution sample; the solution samples were used only once. In each experiment, the initial voltage was approximately 1.4 V, and the voltage fell to approximately 0 V as the aluminum coating was exposed to the fluoride solution.

*Software and Graphing*

The software LabVIEW was used on the PC to run and record the experiments; the output voltage was recorded in an excel spreadsheet containing a time stamp and the magnitude of the voltage. The excel spreadsheets containing the time stamp and voltage were input into a Python script which output graphs and slopes of the experiments. This Python code was written by our lab group for this purpose.

## Results

*Discrepancy in Aluminum Thickness from Sputter Deposition Method*

Sputter deposition was used to coat a thin film of aluminum (Al) on the tips of single mode optical fibers. Sputter deposition uses a vapor-based physical deposition method to deposit thin-films onto a surface [14]. Process parameters for sputtering are limited and consist primarily of controlling the substrate temperature and the gas pressure [15]. An additional process parameter is the distance between the substrate and the target [16].

Common materials to be coated by sputter deposition lay flat across the top of the substrate within the sputter deposition chamber. The substrate is where the material goes that is to be coated with a thin film, and the target is the material that is ionized by high energy sputtering gas atoms and coats the samples on the substrate. We need the tips of the optical fibers to be perpendicular to the surface of the target, meaning the fibers cannot lay flat across the top of the substrate.

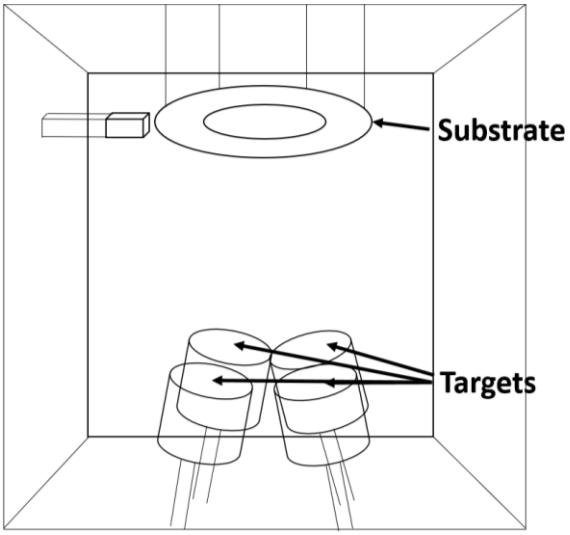


Figure 3.06: The inside of Mantis QUBE sputter deposition chamber. Materials are typically laid flat across the top of the substrate. The targets hold the material or materials that coat the samples laying atop the substrate.

In our previous study [8], fibers were hung by hand through the center of the substrate and vacuum tape was used to secure the fibers in place. Because we had not yet recognized the significance of this parameter, no measurements were taken to ensure the tips of the fibers were the same distance from the target each time the fibers were coated. This led to large variability in the positioning of the fibers during each sputter deposition occurrence. For this reason, we designed a fiber holder to be positioned in the sputter deposition chamber to ensure the tips of the fibers were the same distance from the target each time they were coated [2].

For each round of sputter deposition, we secured up to 17 single-mode optical fibers in the fiber holder. We fixed a 1 $cm^2$ piece of glass to the fiber holder such that the glass was held at the same position as the tips of the optical fibers; the distance between the target and the piece of glass was the same as the distance between the target and the tips of the optical fibers. We intended to sputter coat the optical fibers with 17, 13, and 10 nm of Al. The sputter deposition machine calculated the Al coating thickness at the substrate to be the intended thicknesses. Using a profilometer, we measured the Al thickness on the glass slides to be greater than the intended thicknesses. The results in Table 3.1 show that, due to the proximity of the tips of the optical fibers to the target, we were coating the fibers with, on average, approximately ten times more aluminum than intended.

Table 3.1: Profilometer Data Obtained by Measuring the Al Thickness at 6 or 7 Different Locations on the Glass Slide Sputter Coated Alongside the Optical Fibers Inside the Sputter Deposition Chamber Such That the Glass Slide is Coated With the same Al Thickness as the Tips of the Optical Fibers

| SPUTTER DEPOSITION EVENT | EXPECTED THICKNESS (nm) | ACTUAL THICKNESS PROFILOMETER READINGS (nm) | STANDARD DEVIATION (nm) | AVERAGE ACTUAL THICKNESS (nm) | MAGNITUDE THICKER | AVERAGE MAGNITUDE THICKER |
|---|---|---|---|---|---|---|
| 1 | 17 | 179, 144, 198, 168, 200, 108, 150 | 32.7 | 164 | 9.64x | 9.53x |
| 2 | 13 | 89, 50, 68, 66, 83, 86 | 15.0 | 73.7 | 5.67x | |
| 3 | 17 | 146, 139, 166, 76, 153, 123, 140 | 29.1 | 135 | 7.92x | |
| 4 | 10 | 134, 134, 115, 101, 112, 112, 93 | 15.4 | 114 | 11.4x | |
| 5 | 10 | 158, 125, 269, 77, 82, 69 | 76.1 | 130 | 13.0x | |

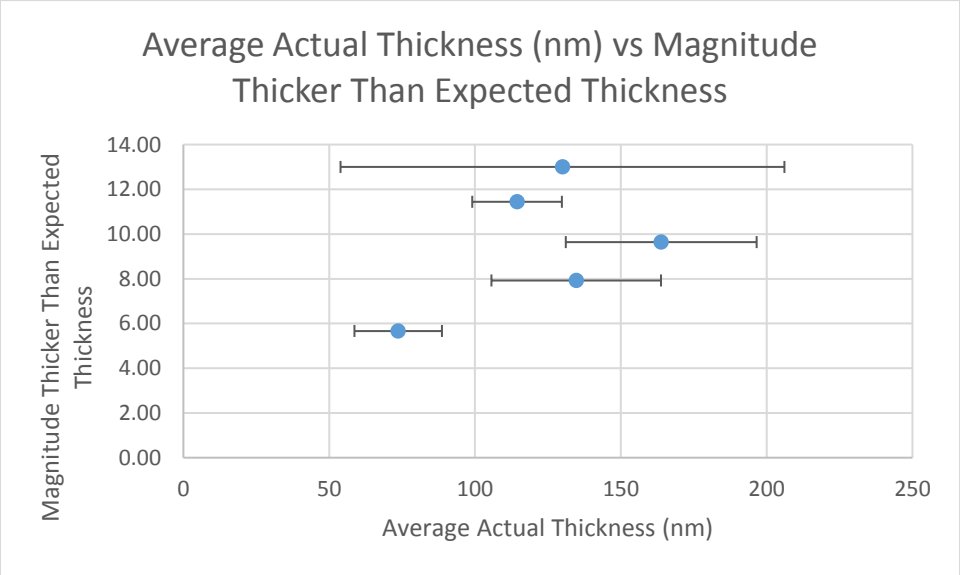


Figure 3.07: Scatter plot depicting the average actual Al thickness on the glass slide (nm) vs the magnitude thicker than expected Al thickness on the glass slide (nm). The error bars represent the standard deviation of the profilometer readings of the Al thickness on the glass slide (nm).

In our initial experiments [8], the software indicated that we coated the fibers with 35 nm of aluminum. We now believe we were coating them with closer to 350 nm of aluminum. Further experiments show the effect of different aluminum coating thicknesses on activation time.

*Aluminum Thickness Effect on Activation Time*

The authors define “activation time” as the time it takes for the output voltage to decrease below 1.2 V. We observed over a large number of experiments that the slope of output voltage is linear between 1.2 and 0.6 V [8], and so we use this definition as a practical metric because it coincides with the beginning of collection of useable data. An example of activation time is shown in Figure 3.08. Once fibers are below the 1.2 V mark, they are said to be “activated”.

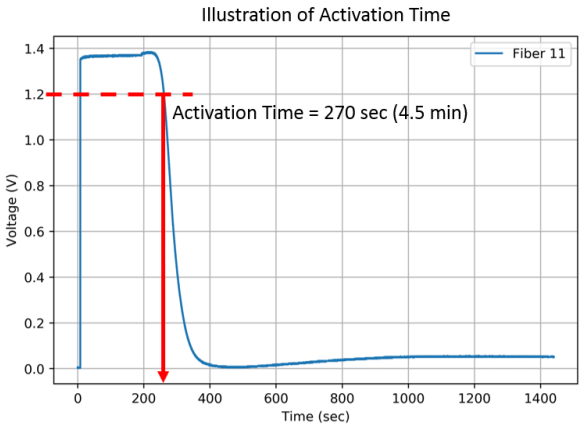


Figure 3.08: Illustration of activation time. For this fiber coated with 35 nm of Al (as indicated by the TITANIUM software) via sputter deposition, the activation time is 270 seconds (about 4.5 minutes).

Our results show that activation time increases as aluminum thickness increases. Table 3.2 shows the average activation time of fibers coated in 5, 9, 9.5, 10, 11, 11.5, 12, 14, 15, 35, 268, and 553 nm of aluminum (as determined by the profilometer) submersed in 5 ppm F- solutions. The activation time of fibers coated in 10 nm of aluminum averages 362 seconds (about six minutes). The activation time of fibers coated with 553 nm of Al is 1514 seconds (about 25 minutes). The trend of aluminum thickness vs activation time is depicted in Figure 3.09a and 3.09b. Figure 3.09b is a zoomed in image of figure 3.09a to better show the trend of fibers coated in 5 to 15 nm of aluminum.

Table 3.2: Average activation times of fibers coated with 5 nm to 553 nm of aluminum in a solution of 5 ppm fluoride pH=7 0.263 mM Ionic Strength

| ALUMINUM THICKNESS (nm) | AVERAGE ACTIVATION TIME (sec) | AVERAGE STANDARD DEVIATION (sec) | NUMBER OF FIBERS (n) | RATE CHANGE OF OUTPUT VOLTAGE (V/sec) |
|---|---|---|---|---|
| 553 | 1514 | 233 | 2 | - |
| 268 | 2103 | 1817 | 6 | - |
| 35 | 5399 | 772 | 14 | -0.00816 |
| 15 | 1149 | 977 | 8 | -0.00978 |
| 14 | 898 | 1244 | 5 | -0.0187 |
| 12 | 1071 | 876 | 5 | -0.0091 |
| 11.5 | 683 | 752 | 10 | -0.0137 |
| 11 | 131 | 151 | 12 | -0.0308 |
| 10 | 317 | 717 | 27 | -0.0137 |
| 9.5 | 140 | 208 | 24 | -0.0512 |
| 9 | 239 | 262 | 10 | -0.0130 |
| 5 | 0 | - | 7 | - |

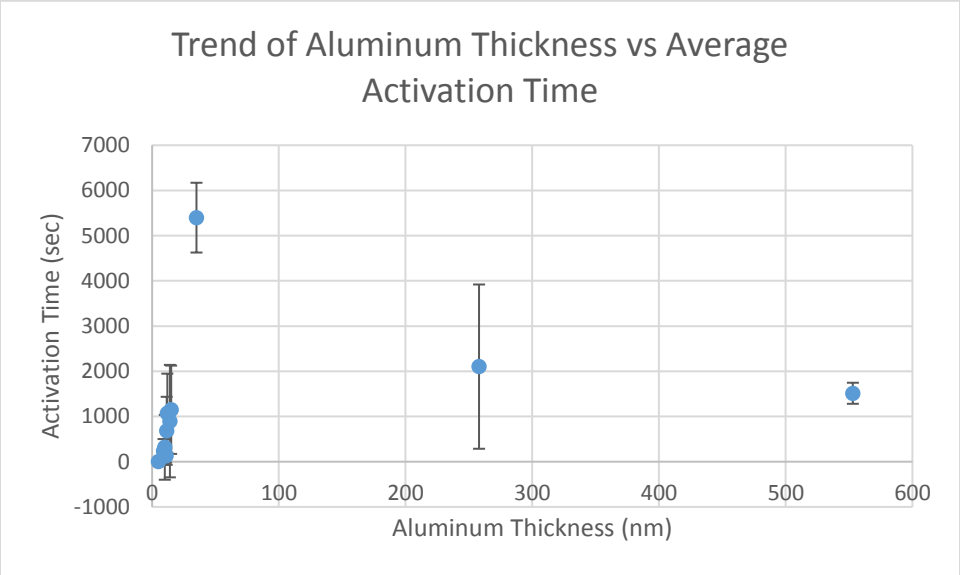


Figure 3.09a: Scatter plot depicting the trend of aluminum thickness vs activation time for fibers coated with 5, 9, 9.5, 10, 11, 11.5, 12, 14, 15, 35, 268, and 553 nm of aluminum (as determined by the profilometer) submersed in 5 ppm F- solutions. The error bars represent the standard deviation.

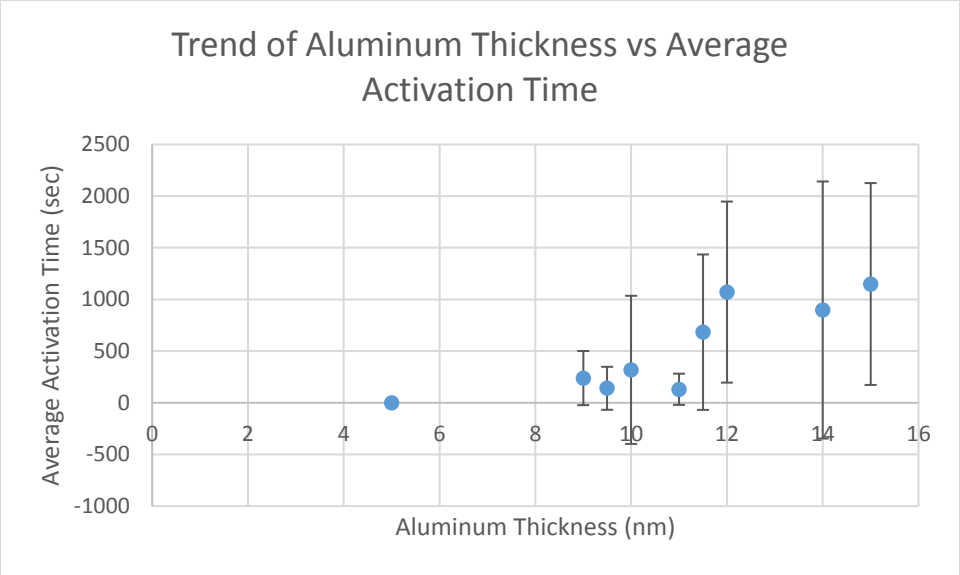


Figure 3.09b: Scatter plot depicting the trend of aluminum thickness vs activation time for fibers coated with 5, 9, 9.5, 10, 11, 11.5, 12, 14, and 15 nm of aluminum (as determined by the profilometer) submersed in 5 ppm F- solutions. The error bars represent the standard deviation.

*Optimal Aluminum Thickness Coating*

Fibers coated with 5 nm of aluminum did not reflect light thus registering no output voltage. Fibers coated with 9 nm and 9.5 nm of aluminum only sometimes registered an initial voltage of 1.4 V. Other times the fibers reflected no light or registered an initial voltage between 0 and 1.4 V; they were not consistent. Fibers that did not show an initial voltage of ~1.4 V are excluded from average activation time calculation in Table 2. The first Al thickness to consistently register a 1.4 V initial output voltage is 10 nm of Al. Since activation time increases as the aluminum thickness increases, 10 nm thus gives the shortest reliable activation time. A thicker Al coating could be used, but for the purposes of our experiments, having longer activation times is not practical.

*Visualization of Aluminum Coatings using Light Microscopy and SEM*

Using a Cytation 5 Plate and Image Reader (BioTek Cytation 5 Cell Imaging Multi-Mode Reader), one may visibly see the difference between aluminum thicknesses. The more aluminum deposited on the optical fibers, the more difficult it is to view the core of the fiber. In figure 3.10, with a coating of 10 nm of aluminum, the core is clearly visible. In figure 3.11 by comparison, the coating of 350 nm of aluminum makes the core difficult to view.

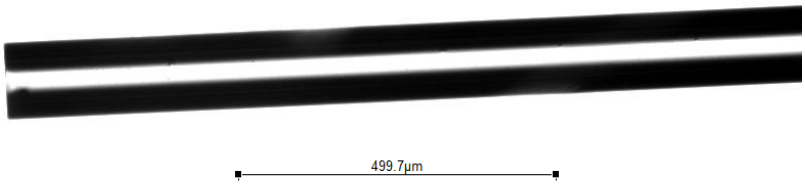


Figure 3.10: Single mode optical fiber coated with 10nm Aluminum. The photo is taken with a Cytation 5 Plate and Image Reader (BioTek Cytation 5 Cell Imaging Multi-Mode Reader) under a 4x APO magnification lens before the fiber was submersed in a fluoride solution.

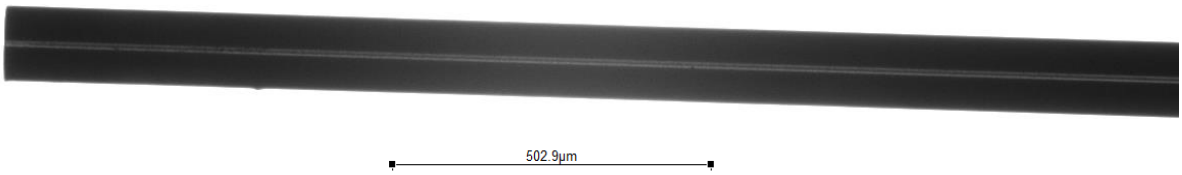


Figure 3.11: Single mode optical fiber coated with 350nm Aluminum. The photo is taken with a Cytation 5 Plate and Image Reader (BioTek Cytation 5 Cell Imaging Multi-Mode Reader) under a 4x APO magnification lens before the fiber was submersed in a fluoride solution.

A scanning electron microscope (SEM) (Hitachi S-4800 FESEM) was used to observe the surface texture of the tips of the optical fibers of an uncoated fiber, before submersion in a fluoride solution, and after submersion in a fluoride solution halfway to completion, and after submersion in a fluoride solution to completion. There are no obvious surface texture differences between the four different SEM images, as can be seen in figures 3.12 to 3.15.

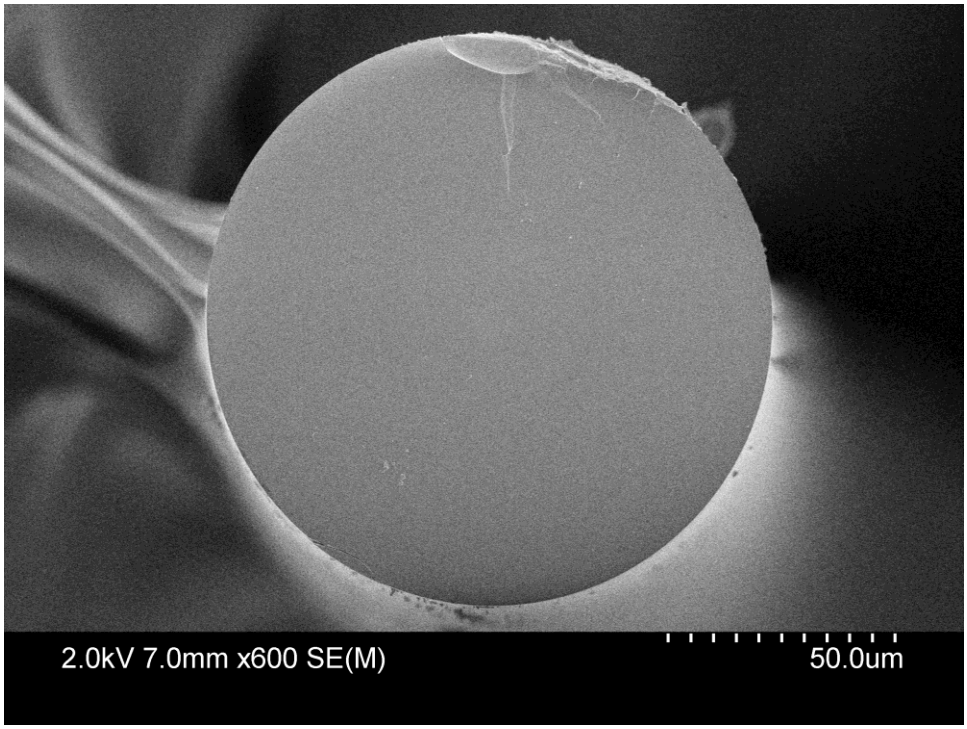


Figure 3.12: SEM image of an uncoated optical fiber using Hitachi S-4800 FESEM

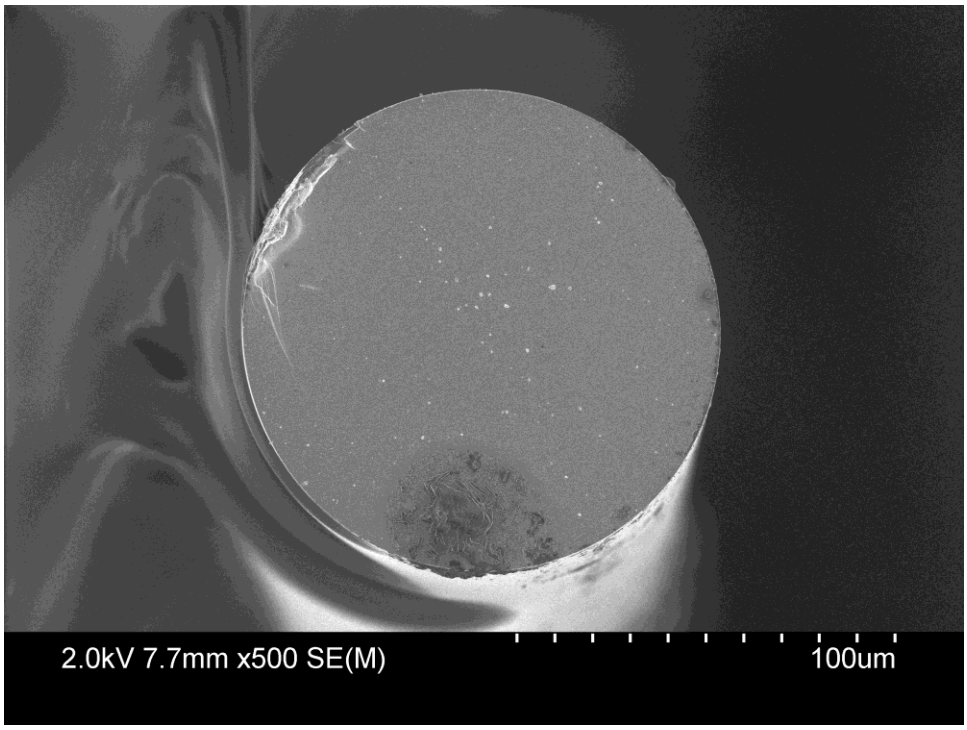


Figure 3.13: SEM image of an optical fiber coated with 35 nm of Al, as measured by the TITANIUM software, using Hitachi S-4800 FESEM

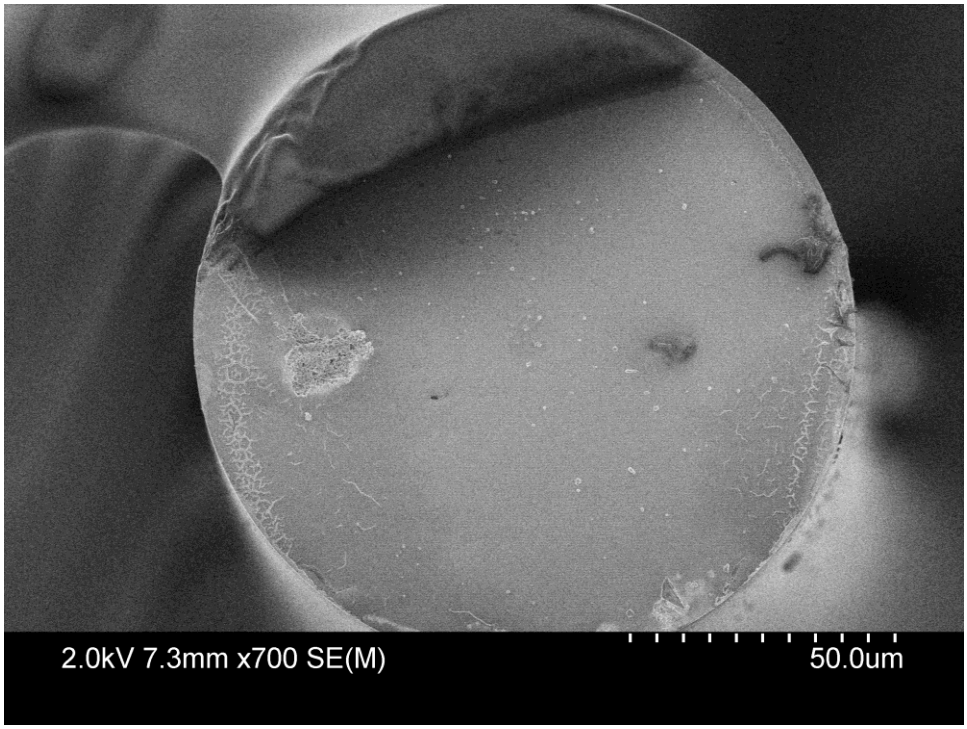


Figure 3.14: SEM image of an optical fiber using Hitachi S-4800 FESEM after being submersed in a 5 ppm F- pH=7 0.263 mM solution and running halfway to completion, meaning the output voltage reached 0.9 V.

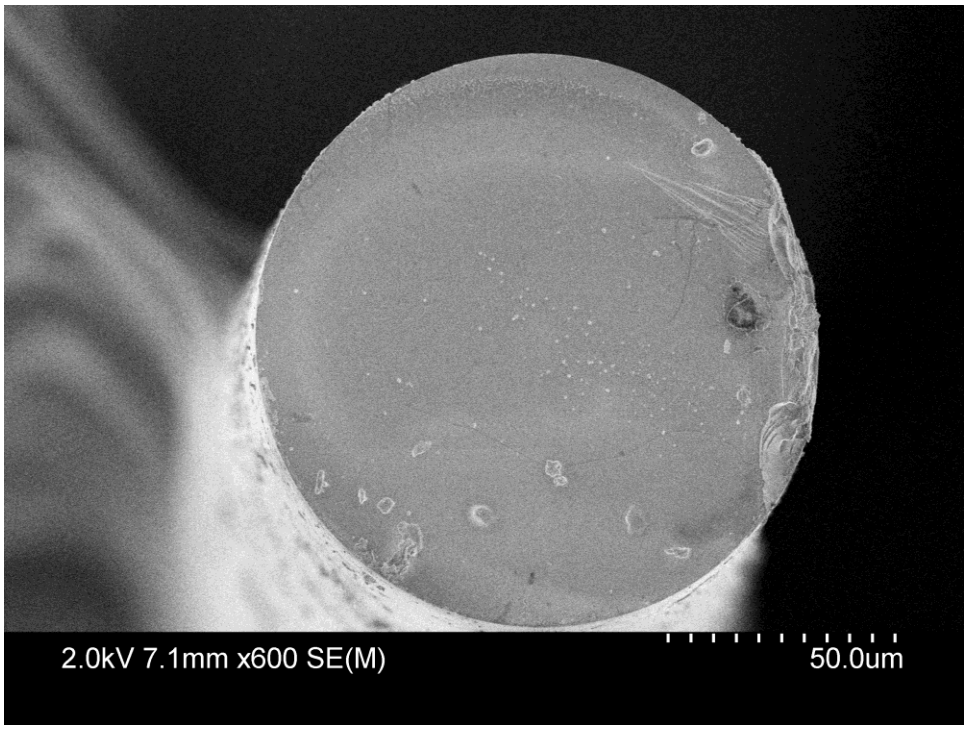


Figure 3.15: SEM image of an optical fiber using Hitachi S-4800 FESEM after being submersed in a 5 ppm F- pH=7 0.263 mM solution and running to completion, meaning the output voltage reached 0 V.

## Discussion

Our experiments with different Al thicknesses lead to the realization that, while the data is noisy, the thickness of the Al coating has an impact on the activation time of the fiber. Over many experiments we concluded that 10 nm of Al is the optimal thickness for decreasing activation time while still sensing fluoride concentrations. Given the lack of control of fiber positioning for sputter deposition in our early work, it is likely that inconsistencies in thickness of Al coating explain the high variability in activation time. We expect the use of the fiber holder to help in coating the desired Al thickness and in ensuring the Al thickness on the tip of the optical fibers is consistent each time we sputter coat. We recommend future work explore the effects of competing ions, temperature, and pH on the rate change of output voltage at different fluoride concentrations.

## Future Work

*Fluoride Concentration Impacts on Rate Change of Output Voltage*

Previous work in our lab group has shown that fluoride concentration impacts the rate change of output voltage [8]. We recommend confirming this observation through the following experiments. We recommend coating fibers with 10, 12, 15, 20, and 35 nm of Al, confirmed with the profilometer, and submersing them in 5 ppm F- and 1 ppm F- solutions. We recommend running five fibers in each solution at each Al coating thickness and averaging the rate change of output voltage for all five fibers. Table 3.3 summarizes the different cases and records the rate change of output voltage.

Table 3.3: Fluoride Concentration Impact on Rate Change of Output Voltage

| Al Coating Thickness (nm) | Solution | Rate Change of Output Voltage (V/sec) | Standard Deviation (V/sec) |
|---|---|---|---|
| 35 | 5ppm F- pH7 0.263mM | | |
| | 1ppm F- pH7 0.0526mM | | |
| 20 | 5ppm F- pH7 0.263mM | | |
| | 1ppm F- pH7 0.0526mM | | |
| 15 | 5ppm F- pH7 0.263mM | | |
| | 1ppm F- pH7 0.0526mM | | |
| 12 | 5ppm F- pH7 0.263mM | | |
| | 1ppm F- pH7 0.0526mM | | |
| 10 | 5ppm F- pH7 0.263mM | | |
| | 1ppm F- pH7 0.0526mM | | |

We hypothesize that, for all Al coating thicknesses, the 5 ppm F- solution has a quicker rate change of output voltage than the 1 ppm F- solution. With data supporting this hypothesis, the conclusion may be drawn that the more fluoride in the water, the quicker the fluoride etches away the Al coating, and the quicker the rate change of output voltage.

Additional future work may explore using an ultrasonic bath to clean the exposed tips of the optical fibers, as well as altering the sputter deposition process by adding a coating of titanium or chromium to the tips of the optical fibers before the Al coating. The purpose of the additional titanium or chromium coating would be to ensure that the Al coating sticks to the optical fiber and does not flake off.

## Conclusion

In this work, a fluoride sensor developed by our group, which is fabricated by coating the tips of single mode optical fibers with a thin film of aluminum and submersion in a fluoride solution has been improved by better controlling the sputter deposition process. We have shown that the thickness of the aluminum coating impacts the amount of time it takes for the sensor to “activate”, thus control of this thickness using a custom-designed fiber holder in the sputter deposition chamber provides a more robust method of coating the fibers. Previous correlation of fluoride concentration and rate of aluminum coating removal remain to be validated under these more controlled conditions. Improvements upon this sensor bring organizations and communities one step closer towards a reagent-free fluoride detection device for in-field measurement.

## Acknowledgements

The authors would like to thank Dr. Jonathan Rudge of the Centre for Advanced Materials and Related Technology (CAMTEC) for his assistance with sputter deposition. Additionally, the authors would like to acknowledge the contribution of coop students Sydney Hoffman and Danika Schmidtke in aiding C.A. Vail in carrying out the laboratory experiments. Thank you to Sydney Hoffman for writing the python code that was used for graphing the data and performing statistical analysis. Furthermore, thank you to coop student Dave Newcombe wrote the LabVIEW code used to run the experiments, and installed the switch with the help of Kevin Jones.

# References


[1] "WHO guidelines for drinking water quality, Vol. 1. Recommendations," World Health Organization, Geneva, 2004.

[2] C. A. Vail, G. Burton, P. M. Wild, and H. L. Buckley, "Fiber Holder to Assist in Sputter Deposition Coating of Optical Fibers," *Submitt. to NHICE Conf.*, 2020.

[3] H. L. Buckley, N. J. Molla, K. Cherukumilli, K. S. Boden, and A. J. Gadgil, "Addressing technical barriers for reliable, safe removal of fluoride from drinking water using minimally processed bauxite ores," *Dev. Eng.*, vol. 3, no. November 2017, pp. 175–187, 2018.

[4] Eawag: Swiss Federal Institute of Aquatic Science and Technology, "Geogenic Contamination Handbook - Addressing Arsenic and Fluoride in Drinking Water," Dübendorf, Switzerland, 2015.

[5] R. Liteplo *et al.*, "Environmental Health Criteria 227. Fluorides.," Geneva, 2002.

[6] G. Rajan, *Optical Fiber Sensors: Advanced Techniques and Applications*. CRC Press, 2015.

[7] M. S. Jadhav, L. S. Laxmeshwar, J. F. Akki, P. U. Raikar, and J. Kumar, "Optical Fiber Technology Fluoride contamination sensor based on optical fi ber grating technology," *Opt. Fiber Technol.*, vol. 38, no. September, pp. 136–141, 2017.

[8] V. Moradi, E. A. Caws, P. M. Wild, and H. L. Buckley, "A simple method for detection of low concentrations of fluoride in drinking water," *Sensors Actuators A Phys.*, p. 111684, 2019.

[9] Y. Wen, D. Kuang, J. Huang, and Y. Zhang, "Microaxicave colour analysis system for fluoride concentration using a smartphone," *RSC Adv.*, vol. 7, no. 67, pp. 42339–42344, 2017.

[10] S. Levin, S. Krishnan, S. Rajkumar, N. Halery, and P. Balkunde, "Monitoring of fluoride in water samples using a smartphone," *Sci. Total Environ.*, vol. 551–552, pp. 101–107, 2016.

[11] E. Vidal, A. S. Lorenzetti, A. G. Lista, and C. E. Domini, "Micropaper-based analytical device (µPAD) for the simultaneous determination of nitrite and fluoride using a smartphone," *Microchem. J.*, vol. 143, no. August, pp. 467–473, 2018.

[12] I. Hussain, K. U. Ahamad, and P. Nath, "Low-Cost, Robust, and Field Portable Smartphone Platform Photometric Sensor for Fluoride Level Detection in Drinking Water," *Anal. Chem.*, vol. 89, no. 1, pp. 767–775, 2017.

[13] HACH, "Fluoride SPADNS Method 8029." pp. 211–217, 2009.

[14] D. Lundin and K. Sarakinos, "An introduction to thin film processing using high-power impulse magnetron sputtering," *J. Mater. Res.*, vol. 27, no. 5, pp. 780–792, 2012.

[15] A. Anders, "Tutorial: Reactive high power impulse magnetron sputtering (R-HiPIMS)," *J. Appl. Phys.*, vol. 121, no. 17, 2017.

[16] R. Wuhrer and W. Y. Yeung, "Effect of target-substrate working distance on magnetron sputter deposition of nanostructured titanium aluminium nitride coatings," *Scr. Mater.*, vol. 49, no. 3, pp. 199–205, 2003.

# Chapter 4

*Manuscript Title*

Integration of an Optical Fiber Switch to Allow Parallel Sensor Development Experiments

*Authors*

C.A. Vail, D. Newcombe, P.M. Wild, H.L. Buckley

*State of Publication:*

This manuscript is intended to be submitted as a Journal Article in the *Journal of Optical Fiber Technology*.

*Author Contributions:*

P.M. Wild suggested the integration of the switch into the experimental setup. D. Newcombe wrote the LabVIEW code that controls the switch. C.A. Vail carried out laboratory experiments and performed statistical analysis of the data. C.A. Vail, P.M. Wild, and H.L. Buckley contributed to the interpretation of the results. C.A. Vail wrote the manuscript; H.L. Buckley provided critical revisions and feedback. H.L. Buckley secured the funding for this project.

## Abstract

Our lab group is developing a reagent-free fluoride sensor for the in-field detection of fluoride concentrations in groundwater [1]. We use single-mode optical fibers in conjunction with a bench-top experimental set-up. Initially, only one optical fiber could be run at a time with the experimental set-up, and we looked to increase the number of optical fibers that could be run at once. In this research, we implement an optical switch into the experimental set-up to allow multi-channel recording of output voltage. We do so by building a LabVIEW code to control the switch and run multiple channels at once. Analysis of our data shows inconsistent slopes in the time vs voltage graphs, and the authors make recommendations for future work.

## Keywords

- Drinking water
- Fluoride
- Sensor
- Optical Switch

## Introduction

Research in our lab group is focused on building a fluoride sensor to test for fluoride concentrations in groundwater [1]. The purpose of the sensor is to allow organizations and communities to make informed decisions about their drinking water, and in turn increase public health. The model of this fluoride sensor is to be reagent-free, portable, reliable, and cost-effective [1]. To achieve this, we are using single-mode optical fibers coated with a thin film of Al to detect fluoride concentrations [1].

Originally, the experimental set-up for the bench-scale sensor used for research and development allowed only one optical fiber to be run at once. This was not time-effective for high throughput over a range of experimental conditions, and we sought solutions on how to increase productivity. The implementation of an optical switch gave us the potential to greatly increase the rate we obtained data. This study focuses on the implementation of the optical switch and the building of LabVIEW code and Python script to managed data collection and data analysis.

## Background

*Use of Optical Switches*

Optical switches were initially invented to support the growing demand on optical network systems [2]. Fundamentally, the role of an optical switch is to route message information in response to supervisory control signals [2]. The information routed may take many different forms, such as multiplexed data in the optical core network, or lower bit channels in the optical access network [2]. The applications of optical switches are not limited to optical communications, but may also be incorporated into large, multi-processor computers [2].

The function of an optical switch is to route an optical signal delivered by an optical fiber, through an integrated optical circuit, to another optical fiber [2]. Several different methods, relying on different physical mechanisms, exist to perform this function. Different types of optical switches include: electro-optical switches, thermo-optical switches, magneto-optical switches, micro-electro-mechanical (MEMS) systems based optical switches, SOA-based optical switches, switching based on optical nonlinear effects, liquid crystal optical switches, photonic crystal all-optical switches, and others [2].

*LabVIEW Software*

LabVIEW is a graphical programming environment that uses a strictly typed language, meaning the language enforces typing on all data being interacted with [3]. A LabVIEW program is called a Virtual Instrument (VI) and is made up of two windows: the front panel and the block diagram [3]. The front panel serves as the user interface for the LabVIEW program and the block diagram serves as the functional, graphical code [3]. Every time an item is created on one of the windows, a corresponding item appears on the other window [3]. Applications of LabVIEW include testing and measurement, data acquisition, datalogging, instrument control, measurement analysis, and report generation applications [3].

*Python Software*

Python is a programming language first developed in 1990 by Guido van Rossum [4]. Since its conception, Python has grown to be implemented across many sectors including industry, research, science, and the service sector [5]. It is renowned for its easy to learn language and user-friendly interface [5].

*Research Objectives*

The work done in our group uses single mode optical fibers to build a sensor capable of detecting fluoride concentrations in groundwater. The objective of this research is to create an effective implementation of LabVIEW code that allows experimental work to reliably record the voltage rate change while making use of an optical switch. We identify issues with the existing LabVIEW code used in conjunction with the Switch, and upon identifying these issues, we alter the Python script used for graphing to accurately timestamp and analyze our existing data.

## Methods and Materials

*Experimental Set-Up and Instrumentation*

Optical fiber tips coated in aluminum, and test solutions of 0-5 ppm fluoride are prepared as described in Chapters 2 and 3.

As shown in Figure 4.01, for one set of experiments, the coated fiber tips are immersed in the test solutions. The broadband light source (BBS 1550, AFC Technologies) emits 1550 nm light that is transmitted through the optical splitter (BRR-35S, Blue Road Research Inc.) to the optical switch (Fiber-Fiber 1x32 Optical Switch Box, Agiltron). The optical switch channels the light to the coated fiber tips; the switch allows up to thirty-two fibers to be run simultaneously, but for the purposes of our experiments, we run up to eight fibers per set of experiments. Light reflected from the fiber tips is transmitted back through the fibers, optical switch, optical splitter, and to the photodiode (FDP 510, MenloSystems). The photodiode produces voltage proportional to the intensity of reflected light, which is transmitted to the data acquisition (DAQ) module (NI USB-6008, National Instruments) at a rate of 10 Hz. The DAQ module converts the output voltage, which is an analog signal, to a digital signal, which is then read by the PC.

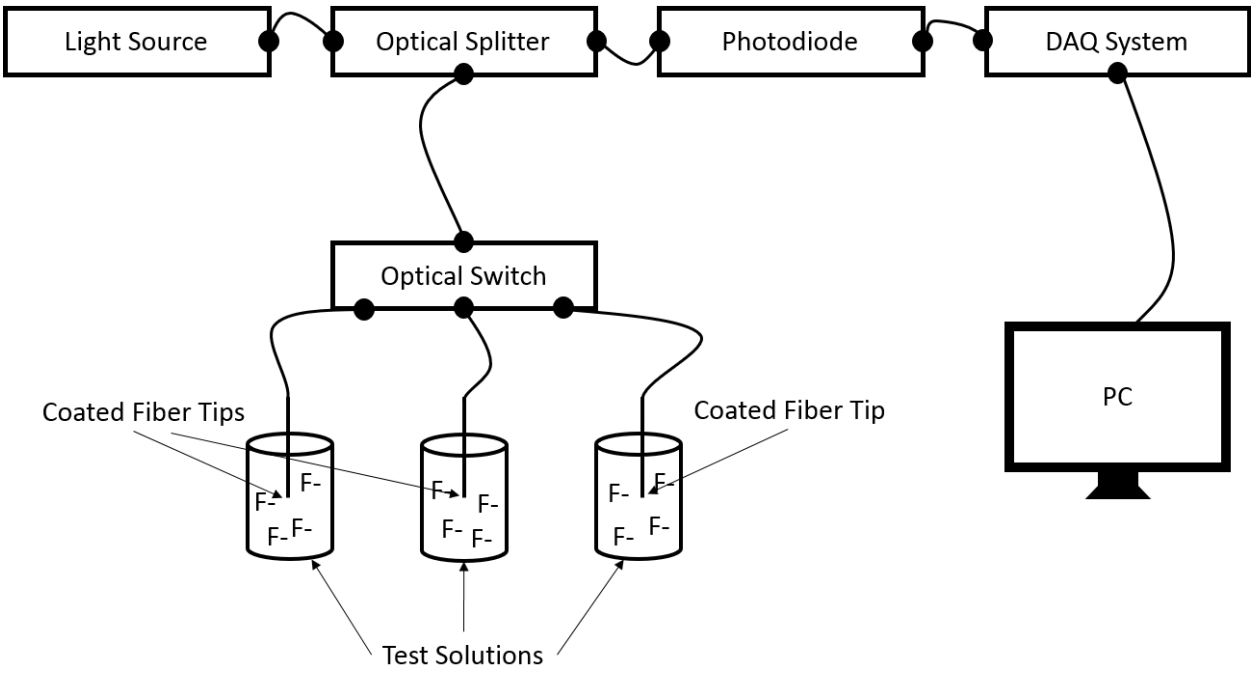


Figure 4.01: Schematic drawing of the experimental set-up as modified from [6].

*Optical Fiber Switch*

The optical switch used in the experimental set-up is a Fiber-Fiber 1x32 Optical Switch Box from Agiltron. The purpose of the optical switch is to connect optical channels so that data can be recorded for more than one fiber submersed in fluoride solutions. Our optical switch accommodates up to 32 channels, but for our experiments we use up to eight channels.

The specification sheet for the optical switch box from Agiltron describes it as an opto-mechanic switch operated by a patent-pending v-grove technology activated by an electric control signal [7]. The specifics of the internal mechanisms of the optical switch are not provided by Agiltron. We could physically open the optical switch box to examine the internal functioning but in doing so we lose the warranty provided by Agiltron. Through examination of the patents, specification sheet, and software code used for controlling the optical switch, we are able to draw some conclusions about the functionality of the optical switch.

The optical switch is controlled through a USB connection with a PC [7]. The PC sends a command to the microcontroller in the optical switch instructing the optical switch which channel to pass light to [7]–[10]. In our experiments we use the software LabVIEW to control the optical switch however, other softwares such as python may be used. There is one input optical fiber into the optical switch and several output channels [7]. The LabVIEW software sends an electric control signal to the microcontroller which in turn activates the solenoid and the stepper motor [7]–[10]. The solenoid pulls the input optical fiber out of the channel it is currently in so it is safe to move, a slight delay occurs, and the stepper motor moves the input optical fiber to align with the next channel [7]–[10]. The solenoid then deactivates, which pushes the input optical fiber into the aligned channel thus transferring light to the output optical fiber [7]–[10]. This mechanism is illustrated in Figure 4.02.

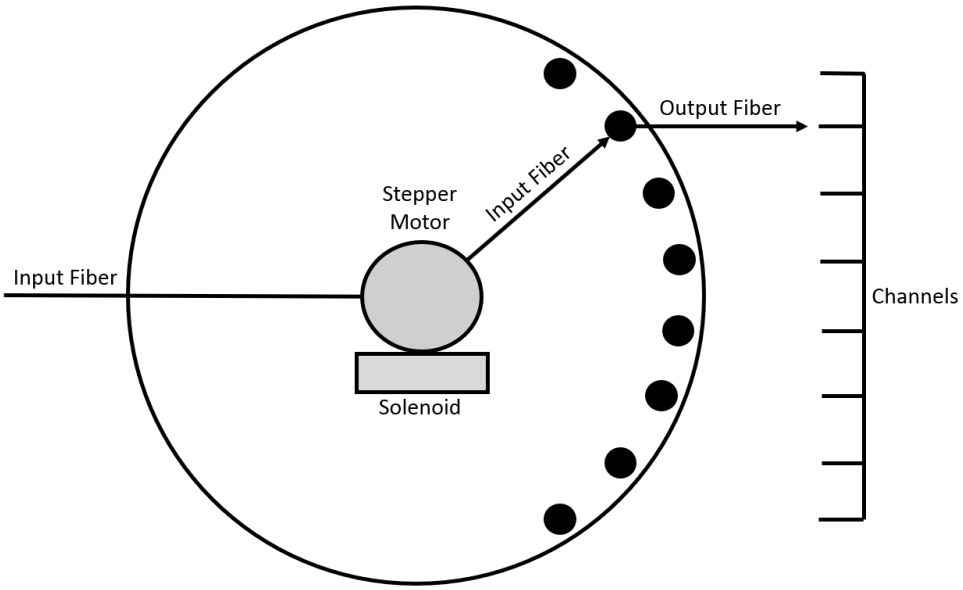


Figure 4.02: Mechanism of the optical switch (Fiber-Fiber 1x32 Optical Switch Box, Agiltron). The LabVIEW code sends an electric control signal to the microcontroller of the optical switch. The microcontroller activates the solenoid and the stepper motor. The solenoid pulls the input fiber out of the channel it currently is in so it is safe to move. A delay occurs and then the stepper motor moves the input optical fiber to align with the next channel. Once the input optical fiber is aligned with the next channel, the solenoid deactivates, thus pushing the input optical fiber into the aligned channel. Light is now transmitted through the input optical fiber to the output optical fiber of that channel.

*LabVIEW Code and Graphing*

A LabVIEW code, written by our lab group for this purpose, is used to control the optical switch and gather multichannel data. The code is written to accommodate eight channels being used by the optical switch. The front panel allows the user to choose which channels on the optical switch to use and displays the graph and voltage of each channel in use.

LabVIEW records the output voltage in an Excel spreadsheet containing a time stamp and the corresponding voltage at that time. The Excel spreadsheets containing the time stamp and voltage are input into a Python script which outputs graphs and slopes of the experiments. This Python script was written by our lab group for this purpose.

## Results

*Initial LabVIEW Code*

The LabVIEW software outputs an Excel spreadsheet containing a time stamp in one column and the corresponding voltage in the next column. A Python script, written by our research group for this specific purpose, is used to graph the data.

The LabVIEW block diagram code written for the implementation of the optical switch was written with the following instructions: two seconds to prepare channel 1, five seconds to record the voltage output for channel 1, two seconds to prepare channel 2, five seconds to record the voltage output for channel 2, etc. This two second, five second routine is repeated for all channels that are set to run, as shown in Figure

4.03. If all eight channels were set to run, this would be, in total, a 56 second cycle. During this 56 second cycle, only five seconds were spent recording an output voltage per channel; there are 51 seconds when data is not being recorded for the given channel.

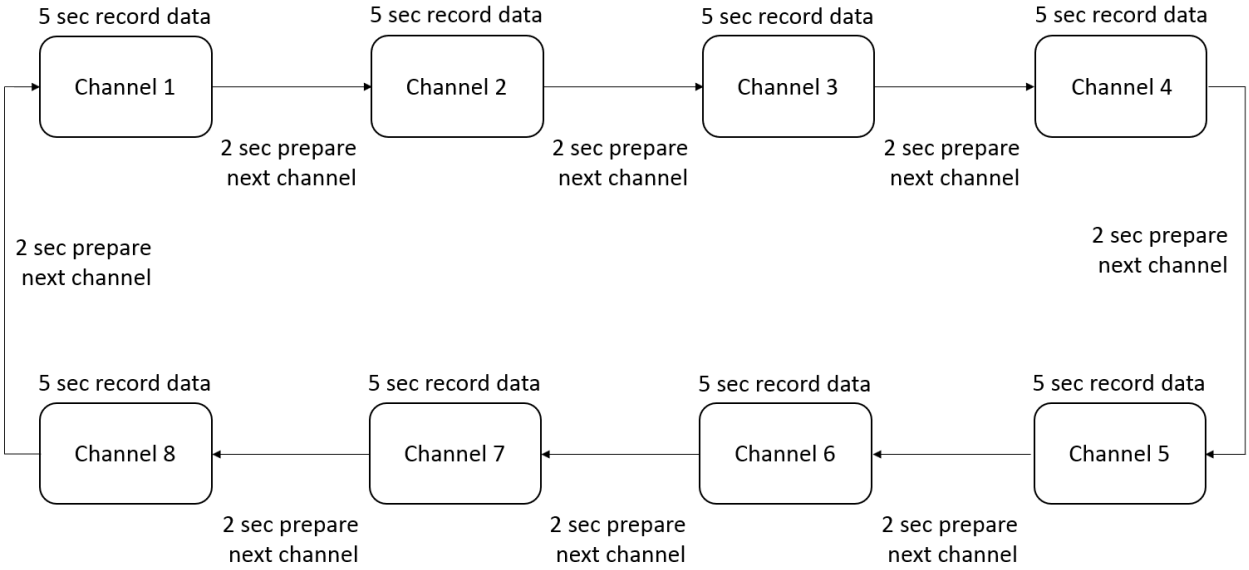


Figure 4.03: Schematic of initial LabVIEW code as designed depicting the 56 second cycle

*Observation of Inconsistent Slopes*

When graphing time vs. voltage, even with data acquired for 5 seconds and then 51 seconds of no data collection, we expected to see a constant slope. One would expect the slope to remain the same because the rate at which the fluoride etches away the aluminum coating is expected to remain constant throughout the experiment and is independent of whether the sample is being measured. Contrary to our expectations, the graphs of time vs. voltage for all experiments conducted using the optical fiber switch showed “steps”, or discontinuities between when the LabVIEW code was recording data compared to when it was not recording data. An example of these steps is shown in Figure 4.04. The graph of Figure 4.4 is zoomed in to show the voltage between 1.2 V and 0.6 V. The slope is visibly steeper when the LabVIEW code is recording data, compared to when it is not. The Python script exports a graph of the fiber, graph of time vs voltage of a fiber submersed in a fluoride solution, a zoomed in graph of time vs voltage between 1.2 V and 0.6 V, as well as an Excel spreadsheet. The Excel spreadsheet contains a slope for each of the “recording data” segments and an average of those slopes.

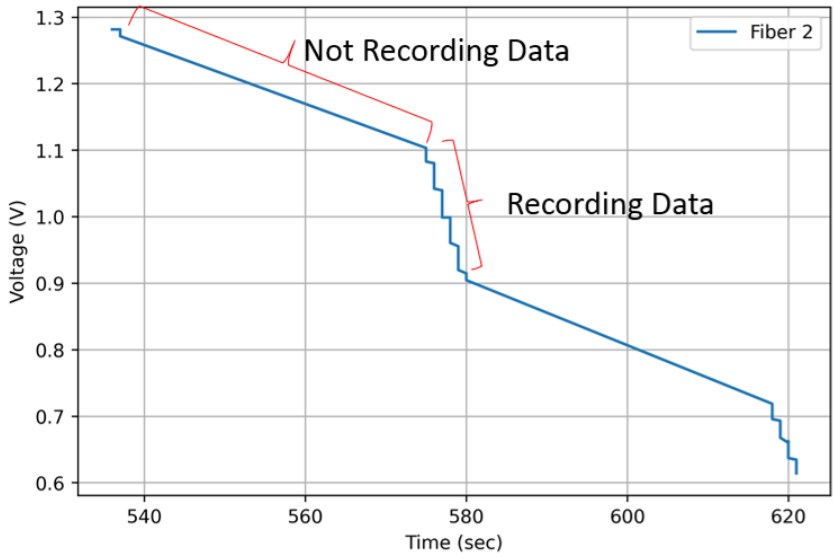


Figure 4.04: Illustration of the change in slope when the LabVIEW code is recording data compared to when it is not recording data. The recording data segments are steeper than the not recording data segments.

*Revised LabVIEW Code*

The LabVIEW code was revised to separate the wait functions from the executable tasks so they each stand in their own frame in the flat sequence structure, as shown in Figure 4.05. The wait functions are important for allowing background functions to execute in a timely function [3]. A flat sequence structure executes each frame in order from left to right until the last frame executes [3]. Putting the wait functions each in their own frame serves to better document the block diagram, decrease parameters that can go wrong with timing, and increase troubleshooting options.

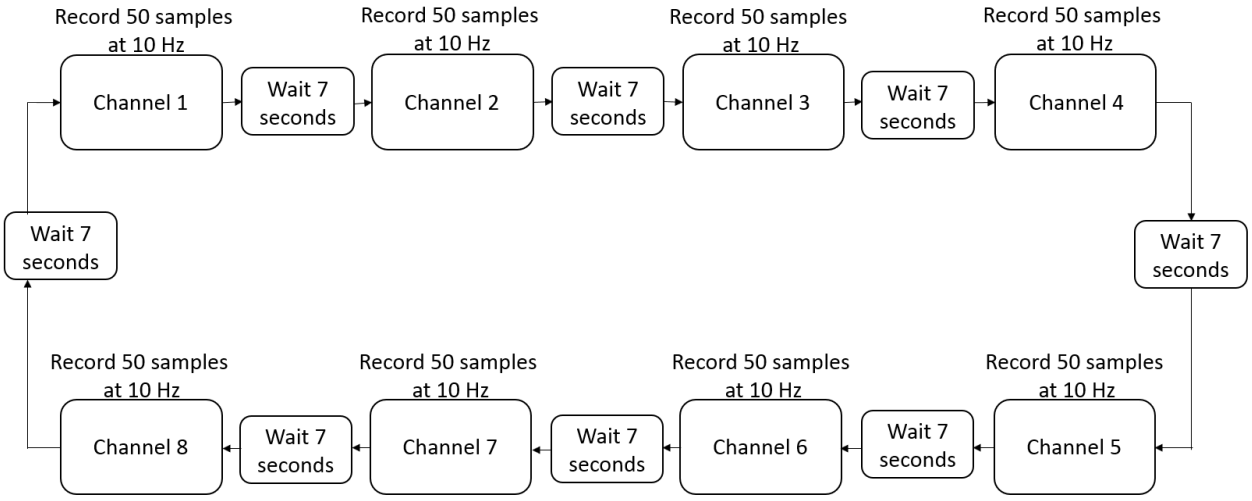


Figure 4.05: Schematic of revised LabVIEW routine

*Continued Observation of Inconsistent Slopes*

Despite the revised LabVIEW code having stricter parameters and more control over the timing sequence, the same inconsistent slopes are still observed, as shown in Figure 4.6.

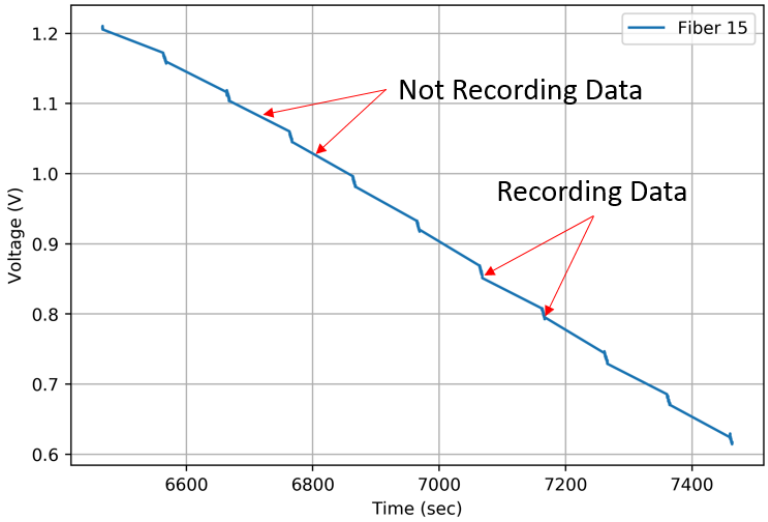


Figure 4.06: Illustration of the change in slope when the revised LabVIEW code is recording data compared to when it is not recording data. The recording data segments are steeper than the not recording data segments.

## Discussion

In summary, the implementation of the optical switch was achieved with the writing of a LabVIEW code. Upon observing inconsistent slopes in the results, revisions were made to the LabVIEW code to allow tighter control of the timing sequence. Despite the revisions to the LabVIEW code, we still observe inconsistent slopes in the graphs of the fibers that were run after the implementation of the optical switch. Data from before the implementation of the optical switch show a constant slope in their graphs, while data collected with the optical switch show steps between collection intervals. We conclude that the implementation of the optical switch is causing the inconsistent slopes. The authors suggest examining the physical characteristics of the optical switch to determine whether the switch itself is causing a spike in output voltage when it switches between channels.

## Conclusion

In conclusion, we have a LabVIEW code that implements the optical switch and records output voltage for up to eight channels. Future work includes examining the physical mechanisms at work within the switch to find a cause for the inconsistent slopes in the graphs. The troubleshooting done in this study brings this research one step closer towards having an effectively implemented optical switch that reliably records output voltage from multiple channels.

## Acknowledgements

The authors would like to acknowledge the contribution of coop students Sydney Hoffman and Danika Schmidtke in aiding C.A. Vail in carrying out the laboratory experiments. Thank you to Sydney Hoffman for writing the Python script that was used for graphing the data and performing statistical analysis. An additional thank you to Kevin Jones for assisting D. Newcombe in the writing of the LabVIEW code and the integration of the switch into the experimental setup.

# References


[1] C. A. Vail, V. Moradi, E. A. Caws, P. M. Wild, and H. L. Buckley, “Development of a Thin-Film Aluminium Coating on the Tip of an Optical Fiber for the Detection of Fluoride in Groundwater,” *J. Sensors Actuators A Phys.*

[2] S. J. Chua and B. J. Li, *Optical Switches: Materials and Design*. Woodhead Publishing, 2010.

[3] I. National Instruments, “LabVIEW User Manual - National Instruments,” no. January. pp. 1–148, 2003.

[4] A. Bell, *Get Programming: Learn to code with Python*. Manning Publications, 2018.

[5] Python software foundation, “Python a programming language changes the world,” 2018.

[6] V. Moradi, E. A. Caws, P. M. Wild, and H. L. Buckley, “A simple method for detection of low concentrations of fluoride in drinking water,” *Sensors Actuators, A Phys.*, vol. 303, 2020.

[7] Agiltron, “SelfAlign ™ 1xN Fiber Optic Switch.” Woburn, MA, 2020.

[8] J. Guanghai, L. Zhang, and J. Zhao, “Patent: Bi-Directional Optical Switch,” US 6,577,430 B1, 2003.

[9] J. Guanghai and J. Zhao, “Patent: None-Mechanical Dual Stage Optical Switches,” US 6,757,101 B2, 2004.

[10] J. Zhao and Y. Shu, “Patent: Multi-Port Optical Switches,” US 2005/0111785 A1, 2005.

# Chapter 5

## Discussion

The aim of this research initially was to prove this fluoride detection method to be sensitive to fluoride concentrations in groundwater up to 5 mg/L of fluoride. While this fluoride detection method has not proven to accurately or precisely detect fluoride concentrations in groundwater, this research has established a robust method of performing experiments using this optical fiber sensing mechanism that will allow for further research that is repeatable, reliable, and capable of drawing conclusive results. This research has tackled the issues of prolonged activation time, unintended and inconsistent aluminum thicknesses, and implementing an optical switch. With this knowledge, we may now move forward to fulfill the initial project aim and prove this fluoride detection method to be capable of sensing fluoride concentrations in groundwater up to 5 mg/L of fluoride. Future work includes testing the fluoride sensor with fluoride solutions containing different pHs, competing ions, and temperatures.

In parallel to this research, we have begun development of a handheld device, about the size of a smartphone, to replace the experimental set-up that allows the optical fiber sensor to be portable into the field. This research is being done by members of our research group with a computer science background. We anticipate this novel fluoride detection method and handheld device to be a solution towards increasing cost-efficiency, ease, and accessibility for in-field fluoride detection.

## Conclusion

This research uses optical fiber technology to create a non-colourimetric, reagent-free fluoride detection device. Over the curse of our experiments, we have strengthened, refined, and improved our methods, materials, and code to create a robust fluoride detection method. Future work of this project includes two streams: testing the fluoride sensor under various conditions and building the handheld device. This fluoride detection device will empower organizations and communities to make informed decisions about their water quality.